# Cell cycle–dependent association of polo kinase Cdc5 with CENP-A contributes to faithful chromosome segregation in budding yeast

Prashant K. Mishra[a], Gudjon Olafsson[b], Lars Boeckmann[a,†], Timothy J. Westlake[a], Ziad M. Jowhar[a], Lauren E. Dittman[a], Richard E. Baker[c], Damien D'Amours[d], Peter H. Thorpe[b], and Munira A. Basrai[a,*]
[a]Genetics Branch, National Cancer Institute, National Institutes of Health, Bethesda, MD 20892; [b]School of Biological and Chemical Sciences, Queen Mary University of London, London E1 4NS, United Kingdom; [c]Department of Microbiology and Physiological Systems, University of Massachusetts Medical School, Worcester, MA 01655; [d]Department of Cellular and Molecular Medicine, University of Ottawa, Ottawa, ON K1N 6N5, Canada

**ABSTRACT** **Evolutionarily conserved polo-like kinase, Cdc5 (Plk1 in humans), associates with kinetochores during mitosis; however, the role of cell cycle–dependent centromeric (*CEN*) association of Cdc5 and its substrates that exclusively localize to the kinetochore have not been characterized. Here we report that evolutionarily conserved *CEN* histone H3 variant, Cse4 (CENP-A in humans), is a substrate of Cdc5, and that the cell cycle–regulated association of Cse4 with Cdc5 is required for cell growth. Cdc5 contributes to Cse4 phosphorylation in vivo and interacts with Cse4 in mitotic cells. Mass spectrometry analysis of in vitro kinase assays showed that Cdc5 phosphorylates nine serine residues clustered within the N-terminus of Cse4. Strains with *cse4-9SA* exhibit increased errors in chromosome segregation, reduced levels of *CEN*-associated Mif2 and Mcd1/Scc1 when combined with a deletion of *MCM21*. Moreover, the loss of Cdc5 from the *CEN* chromatin contributes to defects in kinetochore integrity and reduction in *CEN*-associated Cse4. The cell cycle–regulated association of Cdc5 with Cse4 is essential for cell viability as constitutive association of Cdc5 with Cse4 at the kinetochore leads to growth defects. In summary, our results have defined a role for Cdc5-mediated Cse4 phosphorylation in faithful chromosome segregation.**

**Monitoring Editor**
Kerry S. Bloom
University of North Carolina

Received: Sep 18, 2018
Revised: Jan 4, 2019
Accepted: Jan 30, 2019

## INTRODUCTION

Faithful chromosome segregation is essential for the growth and cellular proliferation of organisms because defects in this process result in aneuploidy, which has been observed in human diseases such as cancer, and developmental disorders (Santaguida and Amon, 2015). A key determinant for high-fidelity chromosome segregation is the kinetochore, which is composed of centromeric (*CEN*) DNA, associated proteins, and a unique chromatin structure (Verdaasdonk and Bloom, 2011; Burrack and Berman, 2012; Musacchio and Desai, 2017). *CEN*s in budding yeast are composed of ~125 base pairs of unique DNA sequence (Clarke and Carbon, 1980), whereas *CEN*s in other eukaryotes are several mega–base pairs of DNA representing sequence repeats, species-specific satellite arrays, or retrotransposon-derived sequences (Verdaasdonk and Bloom, 2011). Despite the *CEN* sequence divergence, the role of *CEN* in chromosome segregation is evolutionarily conserved (Verdaasdonk and Bloom, 2011; Burrack and Berman, 2012). Moreover, many of the ~70 kinetochore proteins representing different subcomplexes from budding yeast (Westermann *et al.*, 2003; Cho *et al.*, 2010; Biggins, 2013) are functionally conserved (Musacchio and Desai, 2017). For example, *CEN* identity in eukaryotic organisms is specified by an epigenetic mark in the form of specialized nucleosomes containing Cse4 (CENP-A in humans, Cid in flies,

This article was published online ahead of print in MBoC in Press (http://www.molbiolcell.org/cgi/doi/10.1091/mbc.E18-09-0584) on February 6, 2019.

†Present address: University Medical Center, 18051 Rostock, Germany.
*Address correspondence to: Munira A. Basrai (basraim@nih.gov).

Abbreviations used: *CAR*, cohesin-associated region; *CEN*, centromere; CF, chromosome fragment; ChIP, chromatin immunoprecipitation; FACS, fluorescence-activated cell sorting; FEAR, Cdc fourteen early anaphase release; FOA, 5-fluororotic acid; GBP, GFP-binding protein; GFP, green fluorescent protein; IP, immunoprecipitation; LC-MS/MS, liquid chromatography–tandem mass spectrometry; PBD, polo-box domain; qPCR, quantitative PCR; RFP, red fluorescent protein; SPI, synthetic physical interaction; YFP, yellow fluorescent protein.

Cnp1 in fission yeast; Sullivan *et al.*, 1994; Stoler *et al.*, 1995; Meluh *et al.*, 1998; Henikoff *et al.*, 2000; Takahashi *et al.*, 2000). In budding yeast, Cse4 contains two distinct domains. The evolutionarily conserved C-terminus histone fold domain (HFD) carries a centromere targeting domain, which is essential for recruitment and incorporation of Cse4 into the *CEN* chromatin (Meluh *et al.*, 1998; Keith *et al.*, 1999). The N-terminus of Cse4 (~129 amino acids) interacts with kinetochore proteins such as the components of the COMA complex (Ctf19, Okp1, Mcm21, and Ame1) and facilitates their recruitment to the *CEN* (Ortiz *et al.*, 1999). Moreover, the N-terminus of CENP-A also directs the targeting of other kinetochore proteins to the *CEN* (Van Hooser *et al.*, 2001). In addition, posttranslational modifications of Cse4, namely, phosphorylation, ubiquitination, sumoylation, methylation, and acetylation also regulate faithful chromosome segregation (Hewawasam *et al.*, 2010; Ranjitkar *et al.*, 2010; Samel *et al.*, 2012; Au *et al.*, 2013; Boeckmann *et al.*, 2013; Ohkuni *et al.*, 2016; Hoffmann *et al.*, 2018). Previous studies have shown that an evolutionarily conserved Ipl1/Aurora B contributes to phosphorylation of Cse4 (Buvelot *et al.*, 2003; Boeckmann *et al.*, 2013). Using mass spectrometric analysis of Cse4 from wild-type yeast cells, we have previously reported the in vivo phosphorylation of Cse4 sites S22, S33, S40, and S105 (Boeckmann *et al.*, 2013). Moreover, a recent study has confirmed the presence of in vivo phosphorylation of Cse4 on serine 33 and shown that *cse4-S33A* mutants show reduced levels of Cse4 at *CEN* when combined with the mutations in histone H2A and H4 (Hoffmann *et al.*, 2018). However, the protein kinase responsible for this modification has not been defined.

Evolutionarily conserved polo-like kinase Cdc5 (Plk1 in humans) regulates several aspects of mitotic cell cycle and chromosome segregation (St-Pierre *et al.*, 2009; Walters *et al.*, 2014; Zitouni *et al.*, 2014) including sister chromatid separation by phosphorylation of Mcd1/Scc1 promoting its proteolytic cleavage by separase (Uhlmann *et al.*, 2000; Alexandru *et al.*, 2001). Cdc5 associates with *CEN* and cohesin-associated regions (*CAR*s) along chromosome arms in a cell cycle–regulated manner and is required for the removal of cohesins from the *CEN* chromatin during mitosis (Rossio *et al.*, 2010; Mishra *et al.*, 2016). In addition to cohesins Mcd1/Scc1 and Smc3, several other Cdc5-interacting proteins have been identified, such as protein kinase Swe1, protein phosphatase Cdc14, spindle pole body components Spc72 and Spc110, and the Cdc fourteen early anaphase release (FEAR) network protein Slk19 (Alexandru *et al.*, 2001; Snead *et al.*, 2007; Park *et al.*, 2008; Rahal and Amon, 2008; Roccuzzo *et al.*, 2015; Botchkarev and Haber, 2018). Moreover, Plk1 in human cells has been shown to phosphorylate kinetochore protein Mis18BP1 to facilitate the assembly of newly synthesized CENP-A at the *CEN* (McKinley and Cheeseman, 2014); however, a homologue of Mis18BP1 has not been identified in budding yeast. Intriguingly, a candidate-based screen using Cdc5 polo-box domain (PBD) as a bait showed an enrichment of kinetochore proteins Cse4 and Tid3 (Snead *et al.*, 2007); however, the molecular significance of the interaction of Cdc5 with Cse4, and Cdc5 substrates that localize exclusively to the kinetochore have not been characterized.

In this study, we show that Cdc5 interacts in vivo with Cse4 in mitotic cells (G2/M) and phosphorylates Cse4 in vitro and in vivo. Cdc5-mediated Cse4 phosphorylation regulates faithful chromosome segregation as evident from the increased frequency of chromosome loss in the nonphosphorylatable *cse4* mutant (*cse4-9SA)* when combined with a deletion of *MCM21*. Significant reduction in levels of kinetochore protein Mif2 and cohesin Mcd1/Scc1 are observed at *CEN* chromatin in a *cse4-9SA mcm21Δ* strain. The constitutive association of Cdc5 with Cse4 at the kinetochore causes growth defects suggesting that cell cycle–regulated interaction of these two proteins restricted to mitosis is essential for cell viability. In summary, we have identified Cse4 as a substrate for Cdc5 and shown that Cdc5-mediated phosphorylation of Cse4 contributes to high-fidelity chromosome segregation.

## RESULTS

### Cdc5 interacts with Cse4 in vivo in a cell cycle–dependent manner

The budding yeast polo-like kinase, Cdc5, associates with centromeres in mitosis and facilitates the removal of *CEN* cohesin (Mishra *et al.*, 2016). Cse4 was enriched in a screen to identify proteins that interact with the PBD of Cdc5 used as a bait (Snead *et al.*, 2007). We explored the role of the interaction of Cdc5 with Cse4 in faithful chromosome segregation. Immunoprecipitation (IP) experiments were done to determine whether Cdc5 interacts with Cse4 in vivo. We constructed a strain that expresses HA-tagged Cdc5 and Flag-tagged Cse4. IP was done using protein extracts from logarithmically growing asynchronous cultures (Figure 1, A and B). Western blotting showed that Cdc5 interacts with Cse4 in vivo, whereas no signals were detected in a control experiment using an untagged strain (Figure 1C).

To determine whether the in vivo interaction of Cdc5 with Cse4 is cell cycle regulated, IP experiments were performed using cells synchronized in G1 (α-factor treatment), S (hydroxyurea treatment), or G2/M (nocodazole treatment) stages of the cell cycle. The cell cycle synchronization was confirmed by fluorescence-activated cell sorting (FACS; Figure 1A) and examination of nuclear and cell morphology (Figure 1B). In agreement with previous studies (Charles *et al.*, 1998; Mishra *et al.*, 2016), Cdc5 was expressed in S and G2/M phases of the cell cycle, whereas no protein expression was detected in G1 cells (Figure 1C). IP results showed an in vivo interaction between Cdc5 and Cse4 in G2/M cells (Figure 1C). No interaction of Cdc5 with Cse4 was detected in G1 and S-phase cells despite the expression of Cdc5 in S phase (Figure 1C). As expected, no signals were detected in control experiments performed with an untagged strain (Figure 1C). Taken together, these results provide evidence for cell cycle–regulated in vivo interaction of Cdc5 and Cse4 that occurs in mitotic cells.

### Cdc5 phosphorylates Cse4 in vitro

To determine whether Cdc5 phosphorylates Cse4 directly, we performed in vitro kinase assays with radiolabeled ATP using Cdc5 purified from yeast (Ratsima *et al.*, 2011) and Cse4 purified from *Escherichia coli*. Cse4 was radiolabeled in the presence of Cdc5, whereas no signal was observed from control in vitro assays containing purified histone H3 (Figure 2A). We next performed in vitro kinase assay by incubating purified Cse4 either with wild-type Cdc5 or its kinase inactive Cdc5kd protein (i.e., Cdc5-K110M; Ratsima *et al.*, 2011). Radiolabeled Cse4 was detected in the presence of wild-type Cdc5 but not the kinase inactive *cdc5kd* protein (Figure 2B) suggesting that the assay specifically reflects Cdc5-mediated kinase activity toward Cse4.

### Cdc5-mediated phosphorylation of Cse4 occurs largely within the N-terminus of Cse4

To identify Cse4 residues phosphorylated by Cdc5, we performed an in vitro kinase assay as described in Figure 2A, and samples were analyzed by liquid chromatography–tandem mass spectrometry (LC-MS/MS). A total of nine phosphorylated serine sites (S9, S10, S14, S16, S17, S33, S40, S105, and S154) were identified (Figure 3A). Except for S154, which is located within the C-terminus histone fold domain, the remaining eight serine residues are largely clustered within the N-terminus of Cse4. Sequence analysis showed

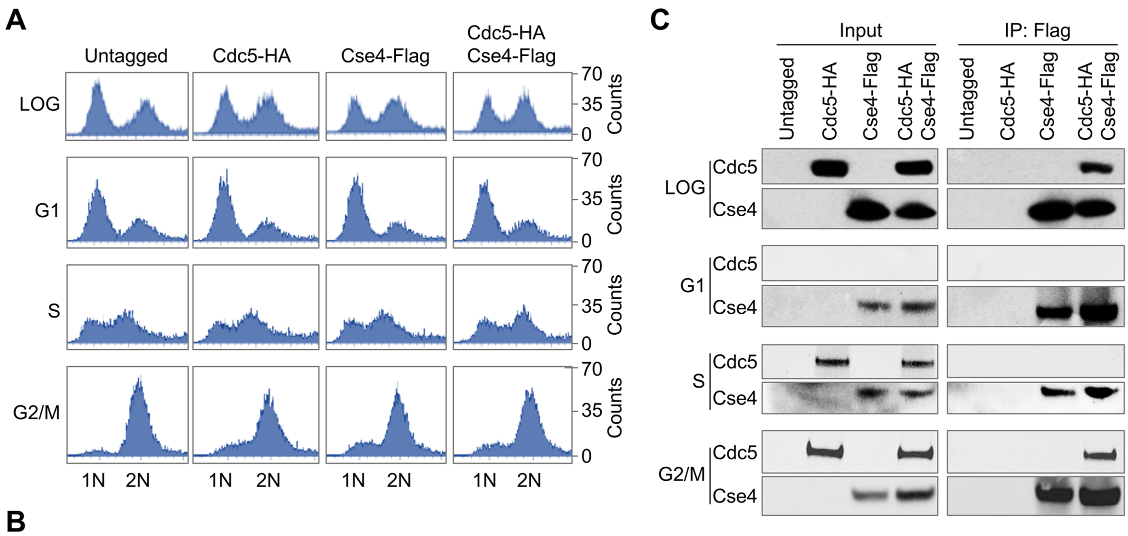


B

| G1 / S / G2/M | Untagged | | | Cdc5-HA | | | Cse4-Flag | | | Cdc5-HA Cse4-Flag | | |
|---|---|---|---|---|---|---|---|---|---|---|---|---|
| | G1 | S | G2/M | G1 | S | G2/M | G1 | S | G2/M | G1 | S | G2/M |
| Asynchronous (LOG) | 36 | 14 | 50 | 32 | 12 | 56 | 25 | 22 | 53 | 29 | 10 | 61 |
| alpha-factor (G1) | 87 | 4 | 9 | 91 | 3 | 6 | 93 | 2 | 5 | 86 | 1 | 13 |
| HU (S) | 9 | 80 | 11 | 7 | 83 | 10 | 3 | 87 | 10 | 7 | 81 | 12 |
| Nocodazole (G2/M) | 3 | 5 | 92 | 8 | 6 | 86 | 9 | 2 | 89 | 4 | 2 | 94 |

**FIGURE 1:** Cdc5 interacts in vivo with Cse4 in a cell cycle–dependent manner. Strains carrying vector control (Untagged, YMB9325), Cdc5-HA (YMB9326), Cse4-Flag (YMB9327), and Cdc5-HA Cse4-Flag (YMB9328) were grown at 30°C to logarithmic phase and synchronized in G1, S, and G2/M stages of the cell cycle. Cell extracts were prepared for immunoprecipitation experiments using α-Flag agarose antibodies. (A) FACS profiles show DNA content in different stages of the cell cycle. (B) Cell cycle stages were determined based on nuclear position and cell morphology by microscopic examination of at least 100 cells for each sample. Different stages of the cell cycle: G1, S phase (S), and mitosis (G2/M). (C) In vivo interaction of Cdc5 with Cse4 is observed in G2/M cells. Immunoprecipitated proteins were analyzed by Western blotting with α-HA (Cdc5), and α-Flag (Cse4) antibodies. IP-Flag represents immunoprecipitated samples.

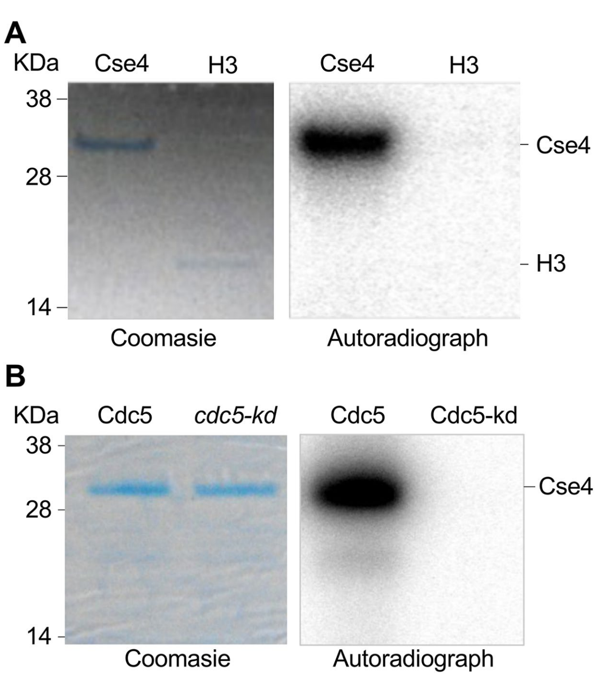


**FIGURE 2:** Cdc5 phosphorylates Cse4 in vitro mediated by its kinase domain. (A) Cdc5 phosphorylates Cse4 in vitro. Kinase assays were carried out in vitro using purified Cse4, Cdc5, and radiolabeled ATP at 30°C for 60 min and products were analyzed by SDS gel electrophoresis followed by Coomassie blue staining and autoradiography of radiolabeled proteins. Purified histone H3 with Cdc5 served as control. (B) Phosphorylation of Cse4 is mediated by the kinase domain of Cdc5. In vitro kinase assays were carried out using purified Cse4, Cdc5, or Cdc5kd (K100M, a kinase-dead variant of Cdc5; Ratsima *et al.*, 2011] and radiolabeled ATP as described above.

that these sites are evolutionarily conserved among different yeast species containing point centromeres (Figure 3B). To explore the physiological effects of the Cdc5-mediated Cse4 phosphorylation, we constructed a phosphorylation-deficient *cse4* mutant, in which all nine phosphorylated serines were changed to alanine (*cse4-9SA*). We examined the ability of *cse4-9SA* to complement the growth of *cse4Δ* strain using 5-fluoroorotic acid (5-FOA)–mediated plasmid shuffle assay (Widlund and Davis, 2005; Tukenmez *et al.*, 2016). Strains carrying *cse4-9SA* grew robustly on 5-FOA plates confirming that *cse4-9SA* allele can complement the *cse4Δ* (Figure 3C). As expected, no growth on 5-FOA was observed in *cse4Δ* strains with a vector used as a negative control (Figure 3C). We next examined the levels of endogenously HA-tagged Cse4 and Cse4-9SA at the *CEN* in a wild-type strain grown at 25°C. ChIP-qPCR (chromatin immunoprecipitation–quantitative PCR) showed that the *CEN* levels of Cse4 and Cse4-9SA were not significantly different (Figure 3D; *p* value > 0.05). No significant enrichment of Cse4 or Cse4-9SA was detected at a negative control non-*CEN HML* locus (Figure 3D).

### Cdc5 contributes to the phosphorylation of Cse4 in vivo

We have previously used α-rabbit polyclonal phospho-Cse4–specific (αp-Cse4) antibodies that did not react with Cse4-4SA in which four serine sites of Cse4 were mutated to alanine (S22A, S33A, S40A, and S105A) to show the occurrence of increased levels of phosphorylated Cse4 at the *CEN* (Boeckmann *et al.*, 2013). Among the four serine sites, three (S33, S40, and S105) are phosphorylated by Cdc5 in vitro (Figure 3A). Hence, we used αp-Cse4 antibody to investigate the role of Cdc5 in Cse4 phosphorylation in vivo. Western blot analysis of affinity-purified Cse4 showed strong reactivity to αp-Cse4 but no signals were detected with Cse4-9SA suggesting that the nine serine residues in Cse4 contribute to the reactivity of Cse4 with αp-Cse4 antibody (Figure 3E). Because we observed an in vivo interaction of Cse4 and Cdc5 in metaphase (Figure 1), we used the αp-Cse4 antibody to examine the in vivo levels of Cse4 phosphorylation in metaphase cells from wild-type and a well-characterized temperature-sensitive *cdc5-99* mutant (St-Pierre *et al.*, 2009). Western blot analysis was done using affinity-purified Cse4 from metaphase cells collected ~110 min after release from G1 arrest into pheromone-free media at 25 and 37°C (Figure 3, F and G). Our results showed similar levels of expression of Cse4 in wild type and *cdc5-99*, both at permissive (25°C) and nonpermissive (37°C) temperature of growth (Figure 3H). The levels of p-Cse4 were similar at 25°C between wild type and *cdc5-99*; however, the levels of p-Cse4 were lower in *cdc5-99* than in the wild-type strain at 37°C (Figure 3H). We quantified the fraction of phosphorylated Cse4 and normalized this to the total Cse4 levels for each sample. The level of phosphorylated Cse4 was significantly lower (~30%) in *cdc5-99* than in the wild-type strain at 37°C (Figure 3I). Taken together, these results indicate that Cdc5 contributes to the phosphorylation of Cse4 in vivo.

### Cse4 phosphorylation-deficient and *mcm21Δ* mutants exhibit synthetic defects in chromosome segregation fidelity

With the exception of one serine, eight of the nine Cse4 serine residues that are phosphorylated by Cdc5 are in the N-terminus of Cse4 (Figure 3A). Cse4 interacts in vivo with Ctf19 and Mcm21 (Ortiz *et al.*, 1999; Ranjitkar *et al.*, 2010), and this interaction is mediated by the N-terminus of Cse4 (Chen *et al.*, 2000). Genetic interactions have also been reported for mutants of *cse4* with *ctf19Δ* and *mcm21Δ* (Samel *et al.*, 2012). Moreover, Mcm21 and Ctf19 have additional roles in maintenance of *CEN* cohesion (Ng *et al.*, 2009; Hinshaw *et al.*, 2017), a biological process in which Cdc5 is also involved (Rossio *et al.*, 2010; Mishra *et al.*, 2016). Because the Cdc5 target sites in Cse4 are clustered largely within the N-terminus of Cse4, we assayed chromosome segregation in *cse4-9SA* strains in combination with deletions of *MCM21* or *CTF19*. The loss of a nonessential reporter chromosome fragment (CF) was measured using the colony color assay as described previously (Spencer *et al.*, 1990). The frequency of CF loss is slightly higher in *cse4-9SA* when compared with the wild-type strain, but the difference is not statistically significant (Figure 4A). The frequency of CF loss in *mcm21Δ* and *ctf19Δ* is significantly higher than the wild-type or *cse4-9SA* strains (Figure 4A). The frequency of CF loss in *ctf19Δ* and *cse4-9SA ctf19Δ* mutant is similar and does not differ significantly from each other (*p* value = 0.3). However, the frequency of CF loss in *cse4-9SA mcm21Δ* mutant is significantly higher than the *mcm21Δ* (~5-fold; *p* value = 0.0023), *cse4-9SA* (~30-fold; *p* value = 0.0009), and the wild-type (~50-fold; *p* value = 0.0008) strains (Figure 4A). These results show that Ctf19-independent events contribute to increased chromosome loss in *cse4-9SA mcm21Δ* strains but do not rule out a role for Cse4 or Cse4-9SA in the loading of Ctf19 to the *CEN* chromatin.

We next examined whether defects in phosphorylation of Cse4-S33 affects chromosome segregation when combined with *mcm21Δ*. The rationale for this experiment is based on our identification of Cse4-S33 as a potential Cdc5 phosphorylation site and a recent study, which showed that phosphorylation-deficient *cse4-S33A* and mutations in histones H2A and H4 exhibit synthetic defects in *CEN* deposition of Cse4 (Hoffmann *et al.*, 2018). The frequency of CF loss in *cse4-S33A* is statistically similar to that observed for wild-type or *cse4-9SA* strains (*p* value = 0.85). However, the frequency of CF loss in *cse4-S33A mcm21Δ* mutant is significantly higher than the *mcm21Δ* (~2-fold; *p* value = 0.021), but is significantly lower than *cse4-9SA mcm21Δ* (*p* value = 0.0094) strains (Figure 4A). Taken together, these results support a role for phosphorylation of Cse4 in faithful chromosome segregation.

### Phosphorylation of Cse4 regulates the *CEN* association of kinetochore protein Mif2 and cohesin component Mcd1/Scc1

Our results for increased chromosome loss in *cse4-9SA mcm21Δ* strains prompted us to examine the role of Cse4 phosphorylation in kinetochore structure. Hence, we examined the levels of *CEN*-associated kinetochore protein Mif2, the yeast orthologue of mammalian CENP-C, which contributes to localization of Cse4 at the *CEN*, maintenance of spindle integrity, and cohesin-based partitioning mechanisms at the kinetochore (Brown *et al.*, 1993; Meluh and Koshland, 1995; Cohen *et al.*, 2008; Ho *et al.*, 2014; Tsabar *et al.*, 2016). ChIP experiments were performed to determine the enrichment of Mif2 at *CEN* and *CARs*: peri-*CEN* (134), chromosomal arm (261), and negative control region (310) on chromosome III in cells synchronized with nocodazole in the G2/M stage of the cell cycle (Figure 4B). No significant enrichment of Mif2 was detected at *CARs* located at peri-*CEN* (134), chromosomal arm (261), or a negative control region (310; Figure 4C). ChIP-qPCR revealed mildly lower levels of *CEN*-associated Mif2 in *cse4-9SA* than the wild-type strain (Figure 4C). However, Mif2 levels at *CEN* were significantly lower in *cse4-9SA mcm21Δ* than the wild-type or single mutant strains (Figure 4C). Western blotting revealed that the reduction in *CEN*-associated Mif2 in the *cse4-9SA mcm21Δ* strain was not due to a reduction in the levels of Mif2 (Figure 4D). On the basis of these results, we conclude that phosphorylation of Cse4 regulates *CEN* association of Mif2 in the absence of Mcm21.

Previous studies have shown that *cse4* and *mcm21Δ* strains exhibit reduced levels of cohesin at the *CEN* and peri-*CEN* chromatin (Weber *et al.*, 2004; Ng *et al.*, 2009). Deletion of *MCM21* results in the failure of Ctf19 loading onto de novo kinetochores suggesting that Mcm21 is required for the assembly or productive association of Ctf19 complex at the kinetochores (Lang *et al.*, 2018). Moreover, defects in levels of *CEN* cohesin have been linked with altered kinetochore function (Brooker and Berkowitz, 2014). Notably, Cdc5 regulates the removal of *CEN* cohesin (Alexandru *et al.*, 2001; Mishra *et al.*, 2016). On the basis of these results, we postulated that defects in Cdc5-mediated phosphorylation of Cse4 may affect *CEN* association of cohesins in an *mcm21Δ* strain. ChIP experiments were performed to examine the enrichment of cohesin component Mcd1/Scc1 at *CEN* and *CARs* in mitotic cells. Mcd1/Scc1 enrichment at chromosomal arm region (261) was similar, and was

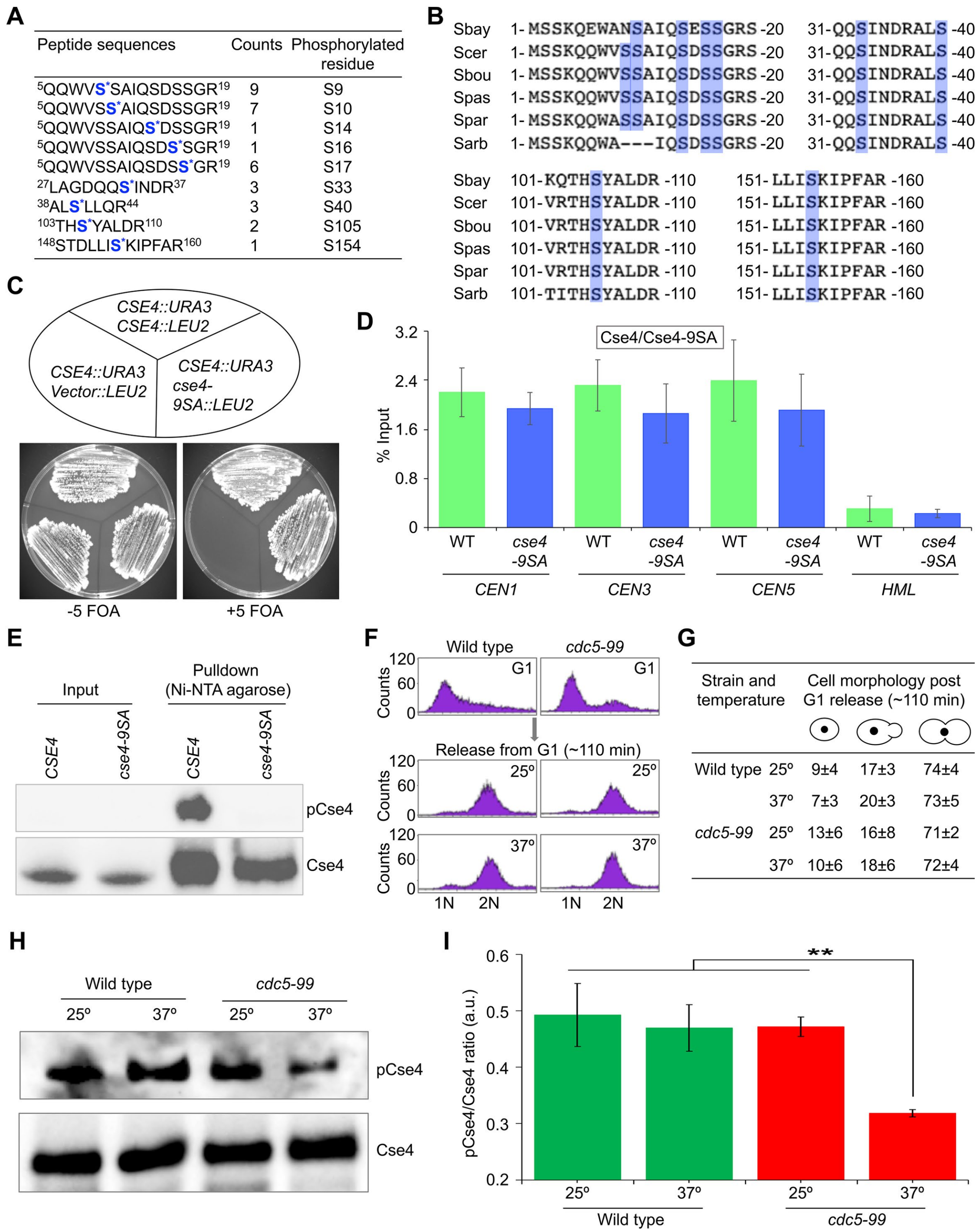


FIGURE 3: Cdc5 phosphorylates Cse4 at its N-terminus in vitro, and contributes to Cse4 phosphorylation in vivo. (A) Cse4 peptides phosphorylated in vitro by Cdc5 were identified by LC-MS/MS. Phosphorylated serines are marked in blue shading. (B) The region containing the phosphorylated serines within the Cse4 (shaded blue) is evolutionarily conserved among yeasts with point centromeres. ClustalW alignment of the Cse4 regions of Sbay = *Saccharomyces bayanus*, Scer = *S. cerevisiae*, Sbou = *Saccharomyces boulardii*, Spas = *Saccharomyces pastorianus*, Spar = *Saccharomyces paradoxus*, and Sarb = *Saccharomyces arboricola*. (C) *cse4-9SA* mutant is viable. Wild-type strain with *CSE4::URA3* (pRB199) was transformed with *vector::LEU2* (YMB10341), *CSE4::LEU2* (YMB10049), or *cse4-9SA::LEU2* (YMB10339). Strains were plated on synthetic medium without or with counterselection for *URA3* by 5-FOA and incubated for 7 d at 25°C. (D) The levels of Cse4 and Cse4-9SA are not significantly different at the *CEN* chromatin. Wild-type (WT; YMB9383) and *cse4-9SA* (YMB10593) strains were grown in YPD to logarithmic phase at 25°C, and ChIP for endogenously expressed HA-tagged Cse4 or Cse4-9SA was performed using α-HA agarose antibodies. Enrichment of Cse4 or Cse4-9SA at *CEN1*, *CEN3*, *CEN5*, and a negative control (*HML*) was determined by qPCR and is presented as percentage of input. The average from three biological replicates ± SE is shown. No statistically significant difference was observed between wild-type and cse4-9SA strains ($p$ value ≥ 0.05; Student's $t$ test). (E) Cse4-9SA protein does not

not significantly different among the strains. No significant enrichment of Mcd1/Scc1 was detected at a negative control region (310; Figure 4E). Enrichment of Mcd1/Scc1 at *CEN* and *CARs* located at peri-*CEN* (134) and chromosomal arm (261) was observed in wild-type and *cse4-9SA* strains (Figure 4E). Significantly reduced levels of Mcd1/Scc1 were observed at *CEN* and peri-*CEN* (134) in a *mcm21*Δ strain (Figure 4E), and this reduction was further exacerbated in *cse4-9SA mcm21*Δ strain in comparison to wild-type, *cse4-9SA*, or *mcm21*Δ strains (Figure 4E). A reduction in enrichment of Mcd1/Scc1 at *CEN* and peri-*CEN* in *cse4-9SA mcm21*Δ strain was not due to a reduction in the protein expression of Mcd1/Scc1 (Figure 4F). On the basis of these results, we conclude that phosphorylation of Cse4 affects the *CEN* association of Mif2 and cohesins during mitosis.

### Centromeric association of Cdc5 regulates *CEN*-associated Cse4 and structural integrity of kinetochores

Cdc5 associates with *CEN* chromatin during mitosis (Mishra *et al.*, 2016), which correlates with the increased levels of phosphorylated Cse4 at the *CEN* (Boeckmann *et al.*, 2013). On the basis of these results, we posit that the absence of Cdc5 from the *CEN* chromatin may exhibit alterations in levels of *CEN*-associated Cse4 and defects in the structural integrity of kinetochores. To address this hypothesis, we assayed the *CEN* association of Cdc5 and Cdc5-99 mutant grown at permissive (25°C) and nonpermissive (37°C) temperatures (St-Pierre *et al.*, 2009). Western blot analysis showed similar levels of expression of Cdc5 and Cdc5-99 at the permissive temperature of 25°C and after a shift to the nonpermissive temperature of 37°C (Figure 5A). ChIP-qPCR showed that the enrichment of Cdc5 and Cdc5-99 at *CEN* chromatin (*CEN1*, *CEN3*, and *CEN5*) is not significantly different at 25°C ($p$ value > 0.05). However, reduced levels of Cdc5-99 were observed at *CEN* chromatin (approximately five- to ninefold) at 37°C (Figure 5B). There was no significant enrichment of Cdc5 or Cdc5-99 at the non-*CEN* negative control region (6K120) relative to that observed at the *CEN* (Figure 5B). Overall, these results show that mutant Cdc5-99 cannot associate with *CEN* at the nonpermissive temperature.

We next examined the effect of loss of *CEN* association of Cdc5-99 on the levels of endogenously HA-tagged Cse4 at the *CEN* using wild-type and *cdc5-99* strains grown at 25°C and after a shift to 37°C. ChIP-qPCR showed that the levels of *CEN*-associated Cse4 in wild-type and *cdc5-99* strains at 25°C are not statistically different ($p$ value > 0.05). However, enrichment of Cse4 at the *CEN* was reduced significantly in *cdc5-99* (1.29% of input at *CEN1*, 1.33% at *CEN3*, and 1.31% at *CEN5*) compared with the levels observed in a wild-type strain (2.49% at *CEN1*, 2.26% at *CEN3*, and 2.42% at *CEN5*) at 37°C (Figure 5C). No significant enrichment of Cse4 was detected at the non-*CEN HML* locus used as a negative control (Figure 5C).

We reasoned that the reduced levels of *CEN*-associated Cse4 in *cdc5-99* strain at 37°C (Figure 5C) may affect the structural integrity of kinetochores. Hence, we used *Dra*I restriction enzyme accessibility assay as described previously to measure the structural integrity of the kinetochore (Saunders *et al.*, 1990; Mishra *et al.*, 2013). DNA was extracted from nuclei prepared from wild-type and *cdc5-99* strains grown at 25 and 37°C after treatment with 100 units of *Dra*I. We quantified the levels of *Dra*I accessibility by qPCR using primers flanking *CEN3* or a non-*CEN* control *ADP1* region (Mishra *et al.*, 2013). The *CEN3* chromatin in *cdc5-99* strain was significantly more susceptible to *Dra*I digestion (approximately twofold) at 37°C than that observed at 25°C (Figure 5D). No significant increased *Dra*I accessibility of *CEN3* chromatin was observed in a wild-type strain at 25 or 37°C (~1.1–1.8%), which was similar to that observed for *cdc5-99* strain at 25°C (~1.4–1.9%; Figure 5D). The *ADP1* chromatin showed low sensitivity to *Dra*I treatments (~1.0–1.3%) and no significant differences in the accessibility of *Dra*I to *ADP1* region were observed between wild-type and *cdc5-99* strains grown at 25 or 37°C (Figure 5D). These results show that *CEN* association of Cdc5 regulates the structural integrity of kinetochores.

### Cell cycle–regulated interaction of Cdc5 with Cse4 is required for cell growth

In vivo interaction between Cdc5 and Cse4 is detectable only in mitotic cells (G2/M; Figure 1C). Hence, we sought to understand the physiological significance of cell cycle–dependent association of Cdc5 with Cse4. We postulated that constitutive association of Cdc5 with Cse4 throughout the cell cycle may affect cell growth. Hence, we used the synthetic physical interaction (SPI) assay (Olafsson and Thorpe, 2015) to examine the effect of constitutive association of Cdc5 with Cse4 at kinetochores. Wild-type Cdc5 protein was linked to the sequence encoding a GFP-binding protein (GBP; Rothbauer *et al.*, 2008), which also carries a tag representing red fluorescent protein (RFP). Plasmids expressing Cdc5-GBP or control-GBP (vector carrying GBP domain) were transformed into strains carrying Cse4-GFP, Cep3-GFP, or non-GFP

react with αp-Cse4 antibodies. Wild-type strains transformed with *GAL1-6HIS-3HA-CSE4* (YMB10426) or *GAL1-6HIS-3HA-cse4-9SA* (YMB10427) were grown to logarithmic phase of growth in synthetic medium, and gene expression was induced in the presence of galactose plus raffinose (2% each) at 25°C for about four generations of growth. Protein extracts were prepared for affinity purification of Cse4 or Cse4-9SA strains using $Ni^{2+}$-NTA agarose. Eluted proteins were analyzed by Western blotting. Antibodies used were α-HA (Cse4) and αp-Cse4–specific (pCse4) antibodies (Boeckmann *et al.*, 2013). (F) Cdc5 contributes to Cse4 phosphorylation in vivo. FACS profiles show G1 synchronization and release into pheromone-free media to enrich cells in metaphase. Wild-type (YMB10986) and *cdc5-99* (YMB10987) strains expressing *GAL1-6HIS-3HA-CSE4* (pMB1601) were synchronized in G1 (1.5 μM α-factor) in 1× SC –URA galactose plus raffinose (2% each) for 2 h at 25°C. Cells were collected, washed with water, and released into pheromone-free 1× SC –URA galactose plus raffinose (2% each) at 25 and 37°C for ~110 min (~70% cells in metaphase). Protein extracts were prepared and affinity purified as described in E. (G) Cell and nuclear morphology of strains from F post-G1 release into pheromone-free media (~110 min) showing enrichment of cells in the metaphase stage of the cell cycle. The average from three biological replicates ± SD is shown. (H) Western blotting shows a reduction of Cse4 phosphorylation in *cdc5-99* at the nonpermissive temperature (37°C). Affinity-purified proteins from strains grown in F were separated on polyacrylamide gels, and transferred to nitrocellulose membranes. Blots were probed with antibodies: α-HA (total Cse4), and αp-Cse4 antibodies (Boeckmann *et al.*, 2013). Three biological replicates were performed. (I) Quantification of relative phosphorylation of Cse4 from Western blots. Ratio of phosphorylated Cse4 (pCse4) to the total Cse4 levels (Cse4) in wild-type and *cdc5-99* strains was calculated. The histogram represents the average of three biological replicates ± SE. **, $p < 0.01$; Student's $t$ test.

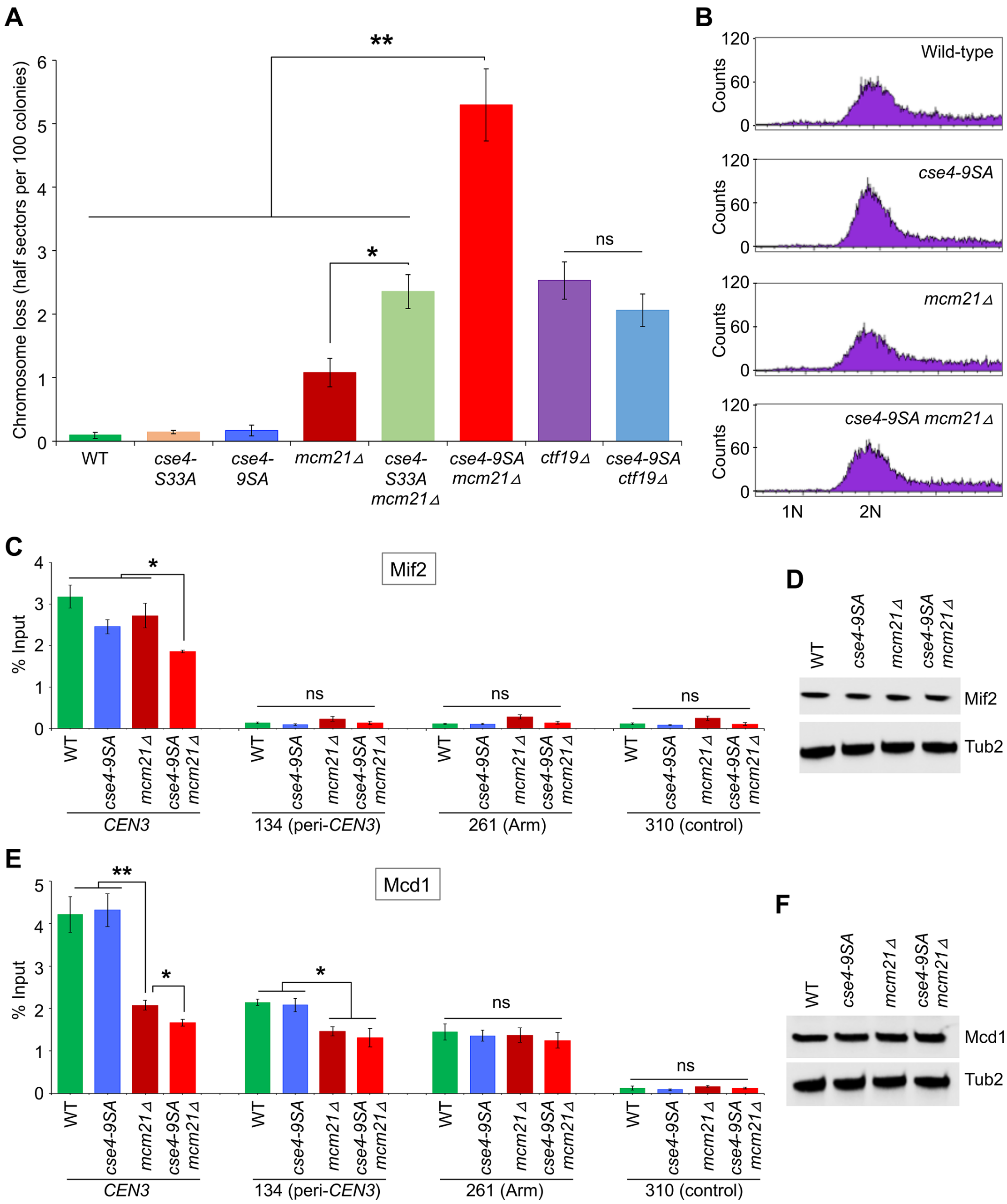


FIGURE 4: Cdc5-mediated phosphorylation contributes to faithful chromosome segregation and modulates the levels of Mif2 and Mcd1/Scc1 at the *CEN* chromatin. (A) Errors in chromosome segregation are increased in *cse4-9SA mcm21*Δ strains. Frequency of CF loss in wild-type (YPH1018), *cse4-S33A* (YMB10984), *cse4-9SA* (YMB10337), *mcm21*Δ (YMB10645), *cse4-S33A mcm21*Δ (YMB10985), *cse4-9SA mcm21*Δ (YMB10646), *ctf19*Δ (YMB10647), and *cse4-9SA ctf19*Δ (YMB10648) strains was determined using a colony color assay as described in *Materials and Methods*. At least 1000 colonies from three independent transformants were counted, and the average from three biological experiments ± SE is shown. **, $p$ value < 0.01; *, $p$ value < 0.05; ns = statistically not significant; Student's $t$ test. (B) The *CEN* levels of Mif2 and Mcd1/Scc1 are reduced in *cse4-9SA mcm21*Δ strains. FACS profiles show DNA content representing the G2/M stage of the cell cycle. Wild-type (YMB9695), *cse4-9SA* (YMB10593), *mcm21*Δ (YMB10740), and *cse4-9SA mcm21*Δ (YMB10741) carrying Mcd1-GFP were grown in YPD to logarithmic phase at 30°C and synchronized in G2/M with nocodazole. ChIP was performed using α-Mif2 antibodies and α-GFP sepharose beads (Mcd1/Scc1) as described in *Materials and Methods*. (C) Enrichment of Mif2 at *CEN3*, *CAR* (134 and 261), and non-*CAR* control region (310) on chromosome III was determined by ChIP-qPCR and is presented as the percentage of input. Average values from three biological replicates ± SE are shown. *, $p$ value < 0.05; ns = statistically not significant; Student's $t$ test. (D) Western blotting showing expression of Mif2 in strains used in ChIP experiments. Antibodies used were α-Mif2 and α-Tub2 (loading control). (E) Enrichment of Mcd1/Scc1 at *CEN3*, *CAR* (134 and 261), and non-*CAR* control region (310) on chromosome III was determined by ChIP-qPCR and is presented as the percentage of input. The average values from three biological replicates ± SE are shown. **, $p$ value < 0.01; *, $p$ value < 0.05; ns = statistically not significant; Student's $t$ test. (F) Western blotting showing expression of Mcd1/Scc1 in strains used in ChIP experiments. The antibodies used were α-GFP and α-Tub2 (loading control).

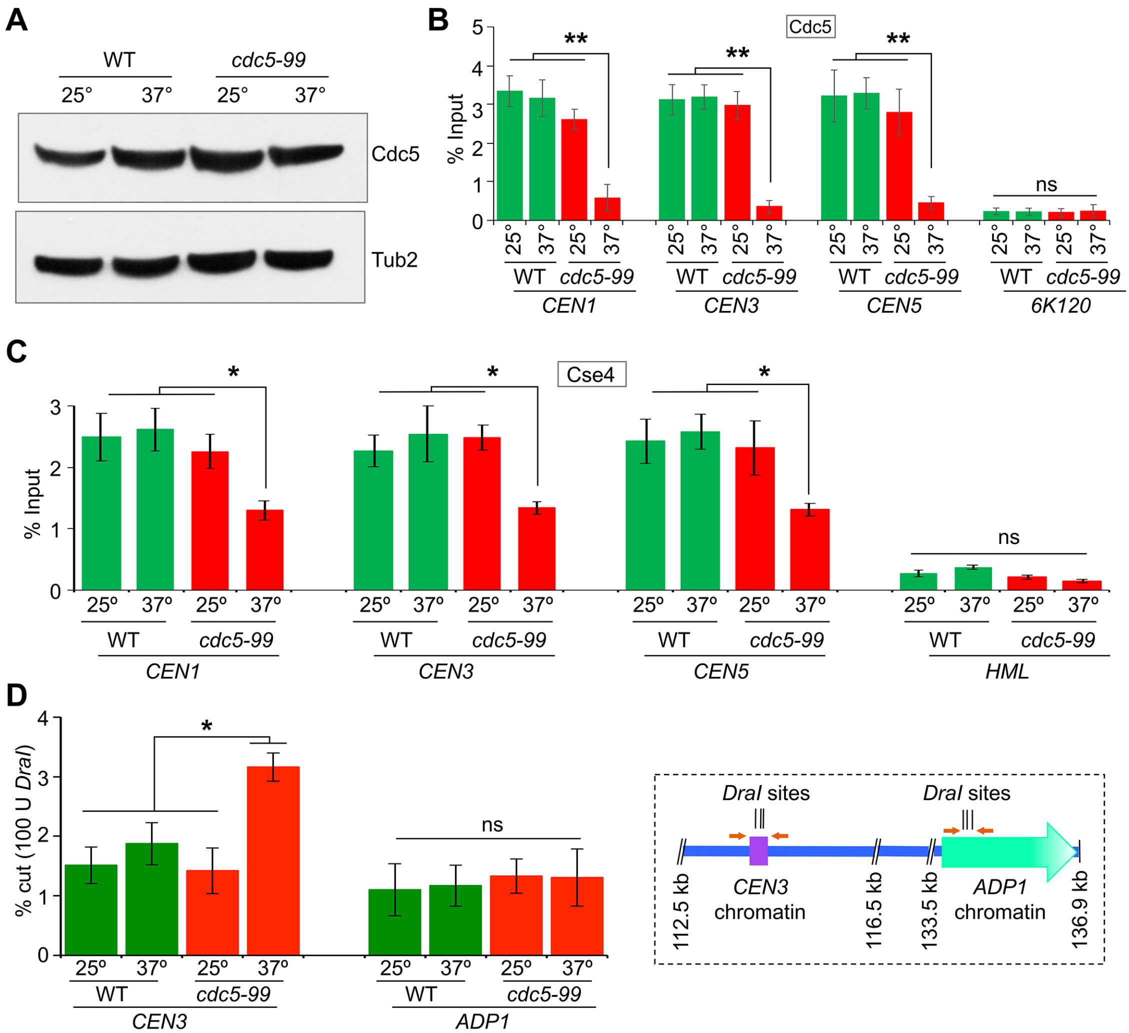


FIGURE 5: Loss of Cdc5 from *CEN* correlates with the reduction in *CEN*-associated Cse4 and defects in structural integrity of kinetochores. (A) Expression of Cdc5 is not affected in *cdc5-99* mutant grown at the nonpermissive temperature (37°C). Wild-type (YMB9431) and *cdc5-99* (YMB9432) were grown to logarithmic phase at 25°C and shifted to the nonpermissive temperature (37°C) for 2.5 h. Whole cell extracts were prepared and Western blots were done using α-Cdc5 and α-Tub2 (loading control) antibodies. (B) Cdc5-99 does not associate with *CEN* at the nonpermissive temperature (37°C) in *cdc5-99* strain. ChIP was performed in strains as described in A using α-Cdc5 antibodies. Enrichment of Cdc5 at *CEN1*, *CEN3*, *CEN5*, and a negative control (6K120) was determined by qPCR and is presented as the percentage of input. The average from three biological replicates ± SE is shown. **, $p$ value < 0.01; ns = statistically not significant; Student's $t$ test. (C) Cdc5 regulates the levels of Cse4 at the *CEN*. Wild-type (YMB9383) and *cdc5-99* (YMB9175) were grown in YPD to logarithmic phase at 25°C and shifted to the nonpermissive temperature (37°C) for 6 h. ChIP for HA-tagged Cse4 was performed using α-HA agarose antibodies. Enrichment of Cse4 at *CEN1*, *CEN3*, *CEN5*, and a negative control (*HML*) was determined by qPCR and is presented as the percentage of input. The average from three biological replicates ± SE is shown. *, $p$ value < 0.05; ns = statistically not significant; Student's $t$ test. (D) Cdc5 is required for the structural integrity of kinetochores. Wild-type (KBY2012) and *cdc5-99* (YMB9367) were grown in YPD to logarithmic phase at 25°C and shifted to nonpermissive temperature (37°C) for 6 h. Nuclei were extracted and incubated with 100 units of *Dra*I restriction endonuclease at 37°C for 30 min as described in *Materials and Methods*. *Dra*I accessibility at *CEN3* and *ADP1* (control) chromatin is shown. The average from three biological experiments ± SE is shown. *, $p$ value < 0.05; ns = statistically not significant; Student's $t$ test. Right inset: schematic modified from our previous study (Mishra *et al.*, 2013) for *CEN3* and *ADP1* regions examined for *Dra*I accessibility.

controls. Microscopic examinations of cells confirmed the colocalization of Cdc5 with Cse4-GFP or Cep3-GFP (Figure 6, A and B). Cep3 is an essential kinetochore protein that binds the *CDEIII* region of the *CEN* (Lechner and Carbon, 1991; Strunnikov *et al.*, 1995) and is ~44 nm away from Cse4 at the metaphase kinetochores (Haase *et al.*, 2013). In control experiment with GBP-RFP, only one or two foci of Cse4 were observed in a cell; however, constitutive association of Cdc5 with Cse4 causes an alteration in its localization pattern as evident from the multiple and diffused Cse4 foci (Figure 6A). Constitutive association of Cdc5 with inner kinetochore protein Cep3, which was used as a control, does not exhibit altered localization phenotype (Figure 6B).

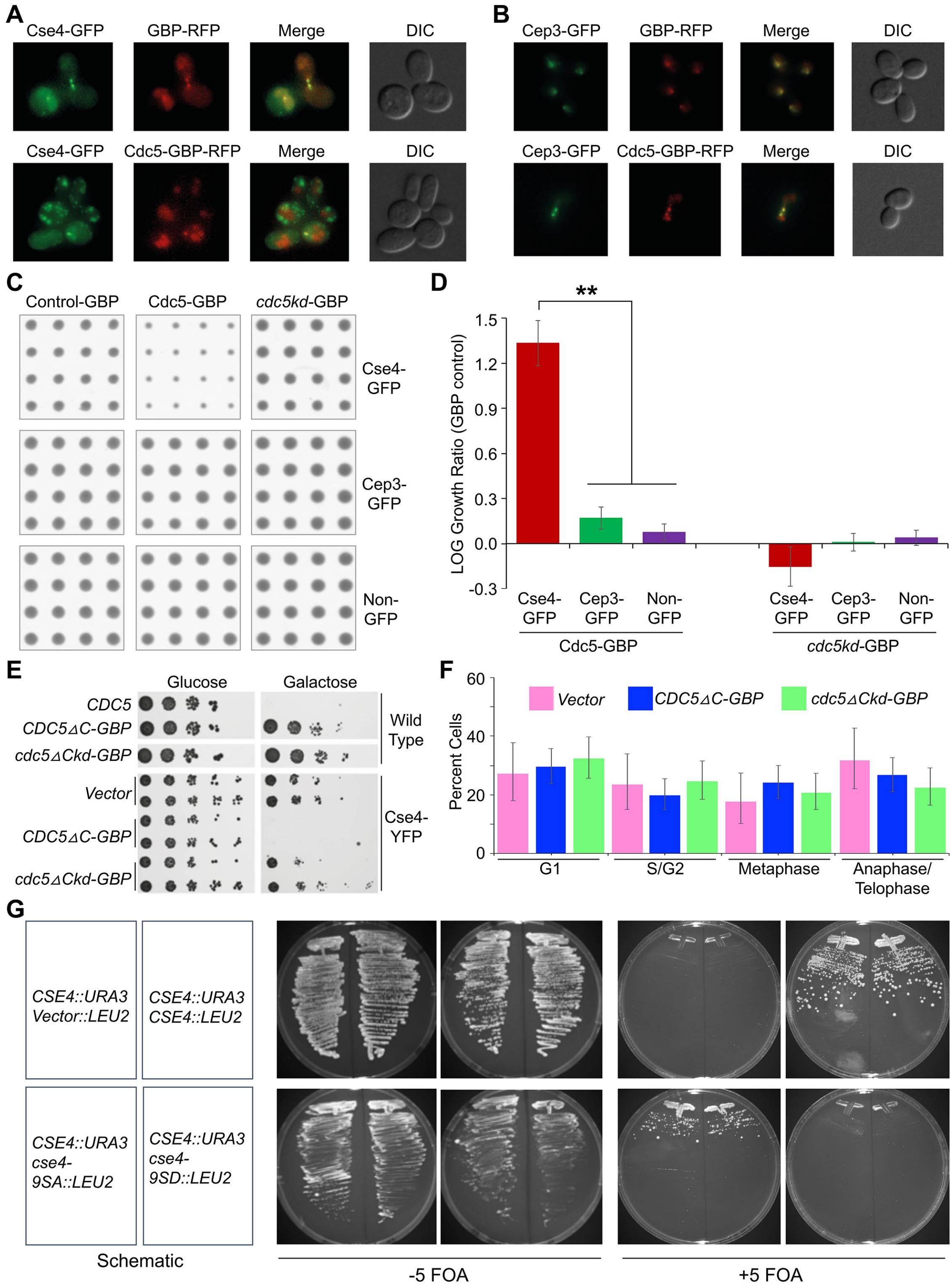


**FIGURE 6:** Cell cycle–regulated interaction of Cdc5 with Cse4 is required for cell growth. A synthetic physical interaction (SPI) assay was performed using plasmids expressing Cdc5-GBP, *cdc5kd*-GBP (kinase-dead version), or GBP alone, which were introduced into Cse4-GFP (internally tagged), Cep3-GFP, and non-GFP strains. (A) The cells from the SPI screen were grown overnight in 1× SC –Leu +Ade with 2% galactose medium at 23°C and imaged using fluorescence microscopy. The GBP-RFP and Cdc5-GBP-RFP signal colocalizes with the GFP signal. Cells with Cse4-GFP and Cdc5-GBP-RFP show multiple Cse4-GFP foci in contrast to Cse4-GFP cells containing GBP-RFP control. (B) Cep3-GFP cells containing either Cdc5-GBP-RFP or GBP-RFP control show normal kinetochore foci; each image is 20.6 μm square. (C) Representative images of the scanned plates from the SPI screen show 16 replicates for each strain (rows) and plasmid (columns) combination. (D) The colony sizes in C were measured and log growth ratios plotted for the GFP and wild-type strains with *pCUP1-GBP* as controls for each comparison. Error bars indicate SD from the

We next performed growth assays using selective ploidy ablation technology (Reid *et al.*, 2011) with 16 replicates per strain to examine the effect of constitutive association of Cdc5 on Cse4. Plates were scanned and growth measurements were determined using the ScreenMill software (Dittmar *et al.*, 2010). Colony sizes were quantified and compared among strains as described previously (Olafsson and Thorpe, 2015). We observed that constitutive association of Cdc5 with Cse4-GFP causes growth defects, whereas no growth inhibition was observed with inner kinetochore protein, Cep3-GFP, or non-GFP control strains (Figure 6, C and D). The growth defects were mediated by the kinase activity of Cdc5 because strains expressing kinase inactive *cdc5kd* exhibited growth phenotypes similar to Cep3-GFP or non-GFP control strains (Figure 6, C and D). To determine whether constitutive association of Cdc5 with Cse4 causes arrest at a particular cell cycle stage, we created conditionally expressed Cdc5 in which the polo-box domain (PBD) was replaced with GBP (*Cdc5ΔC-GBP*) and its kinase inactive mutant (*cdc5ΔCkd-GBP*) under the control of *GAL1* promoter. Cdc5ΔC-GBP was used because overexpression of full-length Cdc5 is lethal. *GALCdc5ΔC-GBP* and *GALcdc5ΔCkd-GBP* were expressed in a wild-type and Cse4-YFP (yellow fluorescent protein) strains. Consistent with the results of the SPI assay, constitutive expression of *Cdc5ΔC-GBP* causes lethality in Cse4-YFP strain, but not in a wild-type strain (Figure 6E). Hence, we assayed the cell cycle stages of *GALCdc5ΔC-GBP* in Cse4-YFP strain after 4 h of growth on galactose. The cell cycle stages categorized based on nuclear position and cell morphology showed that constitutive association of Cdc5 with Cse4 does not cause accumulation of cells in any specific cell cycle stage (Figure 6F). The cell cycle distribution of strains expressing *GALCdc5ΔC-GBP* is not statistically different from *GALcdc5ΔCkd-GBP* or an empty vector control (Figure 6F). To further determine the biological significance of constitutive phosphorylation of Cse4, we constructed the phosphomimetic *cse4* mutant, in which all nine phosphorylated serines were changed to aspartic acid (*cse4-9SD*), and examined its ability to complement the growth of a *cse4*Δ strain after loss of *CSE4/URA3* plasmid by counterselection on medium containing 5-FOA. Strains with Cse4 and *cse4-9SA* grew robustly on plates containing 5-FOA, whereas strains carrying *cse4-9SD* did not exhibit growth on 5-FOA plates after 6 d of incubation at 25°C (Figure 6G). Taken together, these results show that constitutive association of Cdc5 with Cse4 is detrimental to cell growth and define a physiological role for cell cycle–regulated association of Cdc5 with Cse4.

## DISCUSSION

Polo-like kinase Cdc5 and its homologues regulate different stages of the mitotic and meiotic cell cycle and high-fidelity chromosome segregation (Zitouni *et al.*, 2014). Cdc5 in budding yeast associates with the *CEN* chromatin during mitosis (Mishra *et al.*, 2016); however, kinetochore-specific substrates for Cdc5 and the physiological role of Cdc5-mediated phosphorylation of kinetochore proteins have not been characterized. In this study, we have identified Cdc5 as a kinase for Cse4 and defined a role for Cdc5-mediated Cse4 phosphorylation in faithful chromosome segregation. Our results have shown that 1) Cdc5 interacts in vivo with Cse4 in mitotic cells, 2) Cdc5 phosphorylates Cse4 in vitro, 3) Cdc5 contributes to phosphorylation of Cse4 in vivo, 4) mutations that abrogate Cdc5-mediated phosphorylation of Cse4 (*cse4-9SA*) lead to increased chromosome loss, reduction in kinetochore protein Mif2, and cohesin Mcd1/Scc1 at the *CEN* chromatin, 5) constitutive association of Cdc5 with Cse4 at the kinetochore causes growth defects, and 6) mutations that mimic phosphorylation (*cse4-9SD*) lead to loss of viability. We propose that the cell cycle–regulated association of Cdc5 with Cse4 regulates phosphorylation of Cse4 for the structure and function of the kinetochore and cell viability.

In vitro assay showed that the kinase domain of Cdc5 mediates the phosphorylation of Cse4. The failure of Cdc5 to phosphorylate histone H3 implies that in vitro phosphorylation observed is specific to Cse4. Mass spectrometric analysis revealed that nine of the eight serine residues in Cse4 phosphorylated by Cdc5 are within the N-terminus domain of Cse4 (S9, S10, S14, S16, S17, S33, S40, S105). We previously showed in vivo phosphorylation of Cse4 serine sites: S22, S33, S40, and S105 using mass spectrometric analysis of Cse4 from wild-type yeast cells. The phosphorylation of S40 and S105 is regulated by Aurora B kinase Ipl1 in vitro (Boeckmann *et al.*, 2013). Phosphorylation of Cse4 site S33 has been linked with its *CEN* deposition as reduced levels of Cse4 were detected in histone H2A and H4 mutants with phosphorylation-deficient *cse4-S33A* (Hoffmann *et al.*, 2018); however, the kinase responsible for this phosphorylation has not been identified. Our in vitro kinase assay revealed that S33 of Cse4 is a target site for Cdc5 phosphorylation. Moreover, biochemical assays showed that Cdc5 contributes to the phosphorylation of Cse4 in vivo. For example, using αp-Cse4 antibody, we observed a reduction in phosphorylated Cse4 in metaphase cells of a temperature-sensitive *cdc5-99* mutant (St-Pierre *et al.*, 2009). It is notable that a fraction of Cse4 can still be phosphorylated in *cdc5-99* mutant suggesting that this may be mediated by the Ipl1 kinase as reported previously (Boeckmann *et al.*, 2013).

mean. **, $p$ value < 0.01; Student's $t$ test. (E) The forced association of Cdc5 with Cse4 does not arrest cells at a specific cell cycle stage. Tenfold serial dilutions of wild-type and *CSE4-YFP* (T664) strains carrying the *GAL1-CDC5* (pHT573), *GAL1-CDC5ΔC-GBP* (pHT580), *GAL1-cdc5kdΔC-GBP* (pHT581), and *GAL1-Vector* (pHT103) plasmids were spotted onto 1× SC –Leu media containing either 2% glucose (expression OFF) or 2% galactose (expression ON), and grown at 30°C for 2 d. (F) Quantification of the cell cycle stages of the *CSE4-YFP* (T664) strain carrying either the *GAL1-Cdc5ΔC-GBP* or the *GAL1-Vector* and *GAL1-cdc5kdΔC-GBP* control plasmids after growing to logarithmic phase in 1× SC –Leu 2% raffinose media, and then swapped to 1× SC –Leu 2% galactose media for 4 h. The cell cycle stage was assessed by fluorescence microscopy and each cell was counted and given the following cell cycle category: nonbudded cells were categorized as G1 cells, small-budded as S/G2, large-budded cells with two Cse4-YFP foci in the bud neck as metaphase (M), and large-budded cells with completely separated Cse4-YFP foci in the mother and daughter as anaphase/telophase cells. No statistical difference was found between Cdc5ΔC-GBP to either control as evaluated by Fisher's exact test. Error bars indicate 95% confidence interval. (G) *cse4-9SD* mutant is unable to complement the growth defect of *cse4*Δ strain. Wild-type strain with *CSE4::URA3* (pRB199) was transformed with *vector::LEU2* (YMB10341), *CSE4::LEU2* (YMB10049), *cse4-9SA::LEU2* (YMB10339), or *cse4-9SD::LEU2* (YMB10340). Strains were streaked on synthetic medium without or with counterselection for *URA3* by 5-FOA and incubated for 6 d at 25°C.

Together, these data show that phosphorylation of Cse4 is facilitated by at least these two kinases. It is possible that Cdc5 and Ipl1 may regulate differential phosphorylation of Cse4 in response to geometric or conformational changes at the kinetochores during the cell cycle (Pearson *et al.*, 2004; Yeh *et al.*, 2008; Verdaasdonk *et al.*, 2012). This conclusion is consistent with previous reports for multiple protein kinases coordinatively modifying a substrate in response to cell cycle dynamics. For example, Cdc28 and Cdc5 work synergistically for the phosphorylation of Swe1 and condensin in budding yeast (Asano *et al.*, 2005; St-Pierre *et al.*, 2009; Robellet *et al.*, 2015). Moreover, cyclin-dependent kinase (Cdk), meiosis-specific kinase (Ime2), and Cdc5 block DNA replication between the two meiotic divisions by phosphorylation of several components involved in helicase loading and an essential helicase-activation protein Sld2 (Phizicky *et al.*, 2018). Notably, Cdk and Cdc7 kinases function in a concerted manner in phosphorylation of Mcm2 in human cells (Cho *et al.*, 2006). Phosphorylation of S26 and S40 of Mcm2 by both Cdk and Cdc7 kinases have been implicated in DNA replication (Cho *et al.*, 2006).

Our study revealed that the in vivo interaction of Cdc5 and Cse4 is cell cycle regulated and occurs in mitotic cells. The mitotic interaction of Cdc5 with Cse4 is coincident with the cell cycle–regulated association of Cdc5 with *CEN* chromatin in metaphase and early anaphase cells, but lack of enrichment in telophase and G1 cells (Mishra *et al.*, 2016). Notably, the mitotic interaction of Cdc5 with Cse4 also correlates with the increased levels of phosphorylated Cse4 observed at *CEN* in cells arrested in the G2/M stage of the cell cycle but not in G1 (Boeckmann *et al.*, 2013). Taken together, our results show that the phosphorylation pattern of Cse4 overlaps with the *CEN* association and activity of Cdc5 kinase during mitosis (Charles *et al.*, 1998; Alexandru *et al.*, 2001; Hornig and Uhlmann, 2004; Mishra *et al.*, 2016). The cell cycle–dependent phosphorylation of Cse4 is physiologically important because constitutive phosphorylation of Cse4 is detrimental for cell growth as *cse4-9SD* phosphomimetic mutant cannot rescue the growth of a *cse4*Δ strain. Consistent with this hypothesis, we have shown that constitutive association of Cdc5 with Cse4 results in growth defects. We propose that cell cycle–regulated association of Cdc5 facilitates dynamic phosphorylation of Cse4 for the maintenance of proper kinetochore structure and faithful chromosome segregation. Previous studies have shown that dynamic phosphorylation of kinetochore proteins, such as Cse4, Dam1, Ndc80, Dsn1, and Ask1 destabilizes defective kinetochore to promote biorientation by interaction with microtubules (Cheeseman *et al.*, 2002; Westermann *et al.*, 2003; Akiyoshi and Biggins, 2010; Boeckmann *et al.*, 2013; Jin *et al.*, 2017).

A defect in Cse4 phosphorylation (*cse4-9SA*) causes increased errors in chromosome segregation when combined with *mcm21*Δ indicating a role for Cse4 phosphorylation in the maintenance of kinetochore integrity during mitosis. This is not surprising given that *cse4-4SA* and *cse4-S33A* exhibit phenotypic defects only when combined with *dam1* and *hhf1* mutants, respectively (Boeckmann *et al.*, 2013; Hoffmann *et al.*, 2018). Moreover, both Cse4 and Mcm21 have roles in *CEN* structure function, spindle biorientation, and maintenance of *CEN* cohesion (Meluh *et al.*, 1998; Ng *et al.*, 2009; Pekgoz Altunkaya *et al.*, 2016; Tsabar *et al.*, 2016; Mishra *et al.*, 2018). Our results showing significantly reduced levels of Mif2 at *CEN* in *cse4-9SA mcm21*Δ compared with the single mutant (*cse4-9SA* or *mcm21*Δ) further supports a role for phosphorylation of Cse4 in the assembly of *CEN* chromatin and kinetochore function. As *CEN* localization of Mif2 requires Cse4 (Ho *et al.*, 2014), the reduced levels of Mif2 at *CEN* in *cse4-9SA mcm21*Δ strain may be a reflection of altered association of *cse4-9SA* at the *CEN*. A previous study has shown that Mif2 and Cse4 are required for the association of cohesins at the centromeres (Eckert *et al.*, 2007). Moreover, deletion of *MCM21* affects the assembly of Ctf19 complex at the kinetochores (Lang *et al.*, 2018). In agreement with these reports, our results showed reduced levels of Mcd1/Scc1 at the *CEN* in *cse4-9SA mcm21*Δ strains that exhibited a reduction in Mif2 at the *CENs*. We propose that Cdc5-mediated phosphorylation of Cse4 contributes to faithful chromosome segregation.

In summary, we have shown that Cdc5 interacts with Cse4 in vivo in a cell cycle–dependent manner, and this interaction is essential for cell viability. We provide the first evidence for a functional role for Cdc5-mediated phosphorylation of Cse4 in faithful chromosome segregation. It is notable that Plk1 (Cdc5 homologue in humans) phosphorylates kinetochore protein Mis18BP1, which in turn promotes the *CEN* assembly of newly synthesized CENP-A (McKinley and Cheeseman, 2014). However, it remains unexplored whether CENP-A is a direct substrate for Plk1 in human cells. Identification and characterization of additional Plk1 substrates at the human kinetochores will allow us to better understand the role of epigenetic modifications, such as phosphorylation in the assembly of a functional kinetochore for chromosomal stability.

## MATERIALS AND METHODS

### Yeast strains, plasmids, and growth conditions

Yeast strains were grown in yeast peptone dextrose medium (1% yeast extract, 2% bacto-peptone, 2% glucose; YPD) or in synthetic medium with supplements to allow for the selection of plasmids being used. Yeast strains and plasmids are listed in Table 1.

### Chromosome segregation assay

The fidelity of chromosome segregation was measured using a colony color assay as described previously (Spencer *et al.*, 1990). In this assay, the loss of a nonessential reporter CF leads to red sectors in an otherwise white colony. Wild-type, *cse4-S33A*, *cse4-9SA*, *mcm21*Δ, *cse4-9SA mcm21*Δ, *cse4-S33A mcm21*Δ, *ctf19*Δ, and *cse4-9SA ctf19*Δ strains carrying CF were grown in medium selective for the CF to the logarithmic phase, and plated on complete synthetic medium with limiting adenine at 33°C to allow the loss of CF. About 1000 colonies of three transformants were examined for each strain. The frequency of CF loss was determined by counting the colonies that were at least half red representing the loss of the CF during the first mitotic cell division cycle.

### Chromatin immunoprecipitation and qPCR

Chromatin immunoprecipitation (ChIP) experiments were performed with three biological replicates following the procedure as described previously (Mishra *et al.*, 2007, 2011). Antibodies used to capture protein–DNA complexes were α-GFP sepharose (ab69314; AbCam), α-Mif2 (a gift from Pam Meluh, Johns Hopkins University), α-Cdc5 (custom made by the D'Amours laboratory; Ratsima *et al.*, 2011; Robellet *et al.*, 2015), and α-HA agarose (A2095; Sigma Aldrich). ChIP-qPCR was performed in a 7500 Fast Real-Time PCR System using Fast SYBR-Green Master Mix (Applied Biosystems, Foster City, CA) with the following conditions: 95°C for 20 s, followed by 40 cycles of 95°C for 3 s and 60°C for 30 s. The enrichment was determined as percent input using the $_{\Delta\Delta}C_T$ method (Livak and Schmittgen, 2001). Primer sequences are listed in Table 2.

### Cell cycle synchronization, IP, and Western blotting

Strains were grown to logarithmic phase at 30°C in synthetic complete (SC) medium lacking tryptophan (1x SC –Trp) and further incubated for 2 h to synchronize cells in G1 (3 μM alpha factor treatment), S (0.2 M hydroxyurea treatment), and G2/M (20 μg/ml nocodazole treatment) stages of the cell cycle. Cells were collected, washed with water, and grown for 1 h in SC –Trp with galactose + raffinose (2% each) medium to induce the expression of Flag-tagged Cse4 expressed from the *GAL1* promoter. Culture media also contained the chemicals described above to keep the cells in the G1, S, and G2/M stages of the cell cycle. Samples were collected for nuclear morphology, DNA content, and IP analyses. IP experiments were performed using α-Flag agarose antibodies (A2022; Sigma Aldrich) as described previously (Mishra *et al*., 2011, 2018). Whole cell extracts were prepared with the trichloroacetic acid method (Kastenmayer *et al*., 2005), and quantified using Bio-Rad DC protein quantitation assay (Bio-Rad Laboratories, Hercules, CA). Protein samples were resolved on SDS–PAGE and transferred to nitrocellulose membrane. Primary antibodies used for Western blotting were α-HA (H6908; Sigma Aldrich), α-Flag (F3165; Sigma Aldrich), α-GFP (11814460001; Roche), α-Mif2 (a gift from Pam Meluh), and α-Tub2 (custom made by the Basrai laboratory). Secondary antibodies: HRP-conjugated sheep α-rabbit immunoglobulin G (IgG) (NA934V) and HRP-conjugated sheep α-mouse IgG (NA931V) were obtained from Amersham Biosciences (United Kingdom).

### In vitro kinase assay and mass spectrometry

In vitro kinase assay and mass spectrometry were carried out using Cse4 produced and purified from *E. coli* as described previously (Luger *et al*., 1997; Boeckmann *et al*., 2013). Wild-type Cdc5 and its kinase-dead derivative (K100M) were purified from yeast as previously described (Ratsima *et al*., 2011). In vitro kinase assays were performed using radiolabeled ATP in 20-μl reaction volume containing 0.5 μg Cse4, 40 ng Cdc5, 2 mM dithiothreitol, 1 mM $MgCl_2$, 25 mM Tris-HCl, pH 7.5, 100 μM ATP, and 1 μCi of [$\gamma$-$^{32}$P]ATP. Control reactions were performed using purified histone H3 with Cdc5. Reactions were incubated at 30°C for 60 min, stopped with 5 μl of 4× NuPAGE LDS loading buffer (Life Technologies, Grand Island, NY), boiled for 5 min at 95°C, and were run on 4–12% Bis-Tris SDS–PAGE (Invitrogen). Gels were stained with Coomassie blue, and radiolabeled proteins were visualized using a Storm Detector Model 860 (Molecular Dynamics). For mass spectrometry, in vitro kinase assay with and without Cdc5 were performed as described previously (Boeckmann *et al*., 2013). Reactions were analyzed on 4–12% Bis-Tris SDS–PAGE (Invitrogen), and Cse4 bands were excised and subjected to mass spectrometry following the procedures described previously (Waybright *et al*., 2008; Boeckmann *et al*., 2013). The *Saccharomyces cerevisiae* proteome database (www.expasy.org) was used for data analysis.

### In vivo assay for phosphorylation of Cse4

The levels of Cse4 phosphorylation in vivo were determined using procedures and αp-Cse4 antibodies as described previously (Boeckmann *et al*., 2013). Wild-type and *cdc5-99* strains carrying *6HIS-3HA-CSE4* expressed from *GAL1* promoter were grown in 1× SC –URA with 2% glucose media at 25°C. Cells were washed with water and inoculated into 1× SC –URA with galactose + raffinose (2% each) to induce the expression of *6HIS-3HA-CSE4* and 1.5 μM α-factor to synchronize cells in G1. Cells were collected, washed with water, and released into pheromone-free media (1× SC –URA with 2% galactose + raffinose) at 25 and 37°C. Cell cycle progression was monitored by microscopic examination of nuclear and cell morphology. Samples for FACS and affinity pull down were collected ~110 min after G1 release when the majority of cells were at the metaphase (~70%) stage of the cell cycle. Cells were dissolved in lysis buffer (6 M guanidine chloride, 0.5 M NaCl, 0.1 M Tris, pH 8.0) and whole cell extracts were prepared using a FastPrep-24 5G bead beater (40 s, 10 times, 1 min interval between bursts; MP Biomedicals) at 4°C. Whole cell extracts were clarified by centrifugation and incubated with nickel-charged superflow NTA agarose (Qiagen, Valencia, CA) for 16 h at 4°C. Beads were centrifuged and washed once with lysis buffer, followed by three washes with washing buffer (100 mM Tris-Cl, pH 8.0, 20% glycerol, 1 mM phenylmethylsulfonyl fluoride [PMSF]; 5 min each wash at the room temperature). The bound protein was eluted by boiling at 100°C for 10 min in 2× Laemmli buffer with 200 mM imidazole. Protein samples were resolved by SDS–PAGE on 4–12% Bis-Tris SDS–PAGE and transferred to nitrocellulose membranes. Blots were washed with 1× TBST (Tris-buffered saline plus 0.1% Tween 20) three times for 5 min and blocked for 15 min in 1× TBST containing 5% skimmed milk. Western blot analysis was done using primary antibodies: α-HA (1/1000 dilutions; 12CA5; Roche) or αp-Cse4 (1/250 dilutions; Boeckmann *et al*., 2013) in 1× TBST with 5% milk. The secondary antibodies used were HRP-conjugated sheep α-rabbit IgG (NA934V) and HRP-conjugated sheep α-mouse IgG (NA931V). Signal intensities from Western blots were quantified using ImageJ (Schneider *et al*., 2012).

### Extraction of nuclei and *Dra*I accessibility assays

Extraction of nuclei and *Dra*I accessibility experiments were as described previously (Mishra *et al*., 2013) with some modifications. Briefly, cells were dissolved in spheroplasting buffer (20 mM HEPES, pH 7.4, 1.2 M sorbitol, 0.5 mM PMSF), added β-mercaptoethanol (5 μl/ml cell suspension; Sigma Aldrich) and Zymolyase 100T (0.04 mg/ml cell suspension; MP Biomedicals), and incubated at 37°C for spheroplast preparation. Spheroplasting was monitored by measuring $OD_{800}$ in 1% SDS, and reactions were stopped by washing in postspheroplasting buffer (20 mM PIPES, pH 6.8, 1.2 M sorbitol, 1 mM $MgCl_2$, 1 mM PMSF) when >90% spheroplasting was achieved. Spheroplasts were lysed in 20 mM PIPES (pH 6.8), 18% Ficoll 400, 0.5 mM $MgCl_2$, and 1 mM PMSF. Nuclei were released by vortexing for 10 min at 4°C and harvested by centrifugation through a glycerol/Ficoll gradient cushion (20% glycerol, 20 mM PIPES, pH 6.8, 7% Ficoll 400, 0.5 mM $MgCl_2$, 1 mM PMSF). Nuclei were washed and resuspended in *Dra*I buffer (1.0 M sorbitol, 20 mM PIPES, pH 6.8, 0.1 mM $CaCl_2$, 1 mM PMSF, 0.5 mM $MgCl_2$). The nuclei concentrations were determined by measuring $OD_{260}$ in alkaline SDS buffer (0.2 N NaOH, 1% SDS). Equal volumes of nuclei (100 μl) from each sample were prewarmed for 5 min at 37°C followed by the addition of 100 units of *Dra*I (New England BioLabs) for 30 min. Restriction digestion was stopped by adjusting aliquots to 2% SDS, 20 mM EDTA. DNA was isolated after extraction with phenol, chloroform, and isoamyl alcohol (twice), treated with RNase A and proteinase K, followed by extraction with chloroform. DNA was precipitated in ethanol at –20°C, collected by centrifugation, dissolved in 1× TE (pH 8.0), and was used in qPCR to determine the susceptibility of *CEN3* chromatin to digestion by *Dra*I using Fast SYBR-Green Master Mix (Applied Biosystems, CA) and PCR primers flanking *CEN3* and a control region *ADP1* (Mishra *et al*., 2013). The amplification conditions for *CEN3* were initial denaturation at 95°C for 20 s followed by cycling of 95°C for 3 s and 60°C for 30 s (data acquisition step); and for ADP1 the amplification conditions were initial denaturation at 95°C for 30 s followed by cycling of 95°C for 15 s, 54°C for 15 s, and 68°C for 60 s (data acquisition step) in a 7500 Fast Real-Time PCR System (Applied Biosystems, CA). The fraction of DNA cleaved by *Dra*I was determined by normalization of $C_T$ values to those obtained from the no *Dra*I control.

| (A) *Saccharomyces cerevisiae* strains | Genotype | Reference |
|---|---|---|
| YMB9325 | *MATa ura3-52 lys2-801 ade2-101 trp1Δ63 his3Δ200 leu2Δ1 TRP1::CEN URA3::CEN* | This study |
| YMB9326 | *MATa ura3-52 lys2-801 ade2-101 trp1Δ63 his3Δ200 leu2Δ1 CDC5-3HA::TRP1 URA3::CEN* | This study |
| YMB9327 | *MATa ura3-52 lys2-801 ade2-101 trp1Δ63 his3Δ200 leu2Δ1 TRP1::CEN GAL1-FLAG-CSE4::URA3* | This study |
| YMB9328 | *MATa ura3-52 lys2-801 ade2-101 trp1Δ63 his3Δ200 leu2Δ1 CDC5-3HA::TRP1 GAL1-FLAG-CSE4::URA3* | This study |
| YMB10341 | *MATα cse4Δ::kanMX pRS416-CSE4 (pRB199) GAL1-Vector::LEU2* | TianYi Zhang, National Cancer Institute, Bethesda, MD |
| YMB10049 | *MATα cse4Δ::kanMX pRS416-CSE4 (pRB199) GAL1CSE4-3HA::LEU2* | TianYi Zhang |
| YMB10339 | *MATα cse4Δ::kanMX pRS416-CSE4 (pRB199) GAL1cse4-9SA-3HA::LEU2* | This study |
| YMB10340 | *MATα cse4Δ::kanMX pRS416-CSE4 (pRB199) GAL1cse4-9SD-3HA::LEU2* | This study |
| YPH1018 | *MATα ura3-52 lys2-801 ade2-101 trp1Δ63 his3Δ200 leu2Δ1 CFIII (CEN3L.YPH278) HIS3 SUP11* | Phil Hieter, University of British Columbia, Vancouver, BC, Canada |
| YMB10337 | *MATα ura3-52 lys2-801 ade2-101 trp1Δ63 his3Δ200 leu2Δ1 CFIII (CEN3L.YPH278) HIS3 SUP11 cse4-9SA-3HA::URA3* | This study |
| YMB10645 | *MATα ura3-52 lys2-801 ade2-101 trp1Δ63 his3Δ200 leu2Δ1 CFIII (CEN3L.YPH278) HIS3 SUP11 mcm21Δ::kanMX* | This study |
| YMB10646 | *MATα ura3-52 lys2-801 ade2-101 trp1Δ63 his3Δ200 leu2Δ1 CFIII (CEN3L.YPH278) HIS3 SUP11 mcm21Δ::kanMX cse4-9SA-3HA::URA3* | This study |
| YMB10647 | *MATα ura3-52 lys2-801 ade2-101 trp1Δ63 his3Δ200 leu2Δ1 CFIII (CEN3L.YPH278) HIS3 SUP11 ctf19Δ::kanMX* | This study |
| YMB10648 | *MATα ura3-52 lys2-801 ade2-101 trp1Δ63 his3Δ200 leu2Δ1 CFIII (CEN3L.YPH278) HIS3 SUP11 ctf19Δ::kanMX cse4-9SA-3HA::URA3* | This study |
| YMB10984 | *MATα ura3-52 lys2-801 ade2-101 trp1Δ63 his3Δ200 leu2Δ1 CFIII (CEN3L.YPH278) HIS3 SUP11 cse4-S33A-3HA::NAT* | This study |
| YMB10985 | *MATα ura3-52 lys2-801 ade2-101 trp1Δ63 his3Δ200 leu2Δ1 CFIII (CEN3L.YPH278) HIS3 SUP11 mcm21Δ::kanMX cse4-S33A-3HA::NAT* | This study |
| YMB9695 | *MATa MCD1-GFP leu2-3112 ura3-52 his3-11,15 bar1 GAL+ SPC29-RFP::Hyg* | Mishra *et al.*, 2016 |
| YMB10593 | *MATa MCD1-GFP leu2-3112 ura3-52 his3-11,15 bar1 GAL+ SPC29-RFP::Hyg cse4-9SA-3HA::URA3* | This study |
| YMB10740 | *MATa MCD1-GFP leu2-3112 ura3-52 his3-11,15 bar1 GAL+ SPC29-RFP::Hyg mcm21Δ::HIS3* | This study |
| YMB10741 | *MATa MCD1-GFP leu2-3112 ura3-52 his3-11,15 bar1 GAL+ SPC29-RFP::Hyg mcm21Δ::HIS3 cse4-9SA-3HA::URA3* | This study |
| YMB9431 | *MATα ura3-1 leu2-3112 his3-11,15 trp1-1 ade2-1 can1-100 Smc3-GFP::URA3* | This study |
| YMB9432 | *MATα ura3-1 leu2-3112 his3-11,15 trp1-1 ade2-1 can1-100 Smc3-GFP::URA3 cdc5-99::HIS3MX* | This study |
| YMB9383 | *MATa ade2-1 ura3-1 his3-11,15 leu2,3–112 can1-100 CSE4-3HA::NAT* | This study |
| YMB9175 | *MATa ade2-1 ura3-1 his3-11,15 trp1-1 leu2,3–112 can1-100 CSE4-3HA::NAT cdc5-99::HIS3MX* | This study |
| KBY2012 | *MATa trp1Δ63 leu2Δ ura3-52 his3 Δ 200 lys2-8Δ1 CSE4GFP::TRP1 (pKK1) SPC29CFP::kanMX* | Haase *et al.*, 2013 |
| YMB9367 | *MATa trp1Δ63 leu2Δ ura3-52 his3 Δ 200 lys2-8Δ1 CSE4GFP::TRP1 (pKK1) SPC29CFP::kanMX cdc5-99::HIS3MX* | This study |
| W8164-2B | *MATα CEN1-16::Gal-Kl-URA3* | Reid *et al.*, 2011 |
| CEP3-GFP strain | *MATahis3Δ1 leu2Δ0 met15Δ0 ura3Δ0 CEP3-GFP::HIS3* | Huh *et al.*, 2003 |
| T548 | *MATa his3Δ1 leu2Δ0 met15Δ0 ura3Δ0 CSE4-GFP (internal)::HIS3MX6* | This study |

TABLE 1: Strains and plasmids used in this study.

(Continues)

| (A) *Saccharomyces cerevisiae* strains | Genotype | Reference |
|---|---|---|
| BY4742 | *MATα his3Δ1 leu2Δ0 met15Δ0 ura3Δ0* | Resgen |
| T664 | *MATα his3Δ1 leu2Δ0 lys2Δ0 ura3Δ0 CSE4-YFP (internal)::HIS3MX6* | This study |
| YMB10426 | *MATa ura3-1 leu2-3112 his3-11,15 trp1-1 ade2-1 can1-100 GAL1-6HIS-3HA-CSE4::LEU2* (pMB1515) | This study |
| YMB10427 | *MATa ura3-1 leu2-3112 his3-11,15 trp1-1 ade2-1 can1-100 GAL1-6HIS-3HA-cse4-9SA::LEU2* (pMB1847) | This study |
| YMB10986 | *MATa ade2-1 ura3-1 his3-11,15 trp1-1 leu2,3-112 can1-100 GAL1-6HIS-3HA-CSE4::URA3* (pMB1601) | This study |
| YMB10987 | *MATa ade2-1 ura3-1 his3-11,15 trp1-1 leu2,3-112 can1-100 cdc5-99::HIS3MX6 GAL1-6HIS-3HA-CSE4::URA3* (pMB1601) | This study |
| **(B) Plasmids** | **Description** | **Reference** |
| p344 | *CDC5-3HA::TRP1* | D. D'Amours, University of Otttawa, Ottawa, ON, Canada |
| pRB199 | *CSE4-3HA::URA3* | R. Baker, University of Massachusetts Medical School, Worcester, MA |
| pHT4 | *pCUP1-GBP-RFP LEU2* | Olafsson and Thorpe, 2015 |
| pHT425 | *pCUP- CDC5-GBP LEU2* | This study |
| pHT442 | *pCUP1-cdc5kd-GBP LEU2* | This study |
| pHT103 | *pGAL1-empty LEU2* | Olafsson and Thorpe, 2016 |
| pHT573 | *pGAL1-CDC5 LEU2* | This study |
| pHT580 | *pGAL1-CDC5ΔC-GBP LEU2* | This study |
| pHT581 | *pGAL1-cdc5kdΔC-GBP LEU2* | This study |
| pMB1515 | *pGAL1-6HIS-3HA-CSE4 LEU2* | This study |
| pMB1847 | *pGAL1-6HIS-3HA-cse4-9SA LEU2* | This study |
| pMB1601 | *pGAL1-6HIS-3HA-CSE4 URA3* | This study |

TABLE 1: Strains and plasmids used in this study. Continued

| Locus | Forward (5′-3′) | Reverse (5′-3′) | Reference |
|---|---|---|---|
| *CEN1* | CTCGATTTGCATAAGTGTGCC | GTGCTTAAGAGTTCTGTACCAC | Choy *et al.*, 2011 |
| *CEN3* | GATCAGCGCCAAACAATATGG | AACTTCCACCAGTAAACGTTTC | Choy *et al.*, 2011 |
| *CEN5* | AAGAACTATGAATCTGTAAATGACTGATTCAAT | CTTGCACTAAACAAGACTTTATACTACGTTTAG | Choy *et al.*, 2011 |
| *6K120* | AACGTCACTTTTTTTCCAGGG | GCAAAGCTAGCTAACGAACAA | Mishra *et al.*, 2016 |
| *HML* | CACAGCGGTTTCAAAAAAGCTG | GGATTTTATTTAAAAATCGAGAGG | Choy *et al.*, 2011 |
| *CEN3-DraI* | TTGATGAACTTTTCAAAGATGAC | GTCAACGAGTCCTCTCTGGCTA | Choy *et al.*, 2011 |
| *ADP1* | ATCCAAATGTGCTCAAGATAGTAGC | CACCAAACAACATTTACTAGCAGTG | Mishra *et al.*, 2013 |
| *134* | CCGATGGTTAGGATTTCCAACG | GGTTTTCAGAACAGAATGGGGC | Eckert *et al.*, 2007; Ng *et al.*, 2009 |
| *261* | TTGCCACAGCCACAGATATAACTG | GATGGACAAAGCGTTGTATCCG | Eckert *et al.*, 2007; Ng *et al.*, 2009 |
| *310* | TCTCGGAATTTATCATGACCCAT | AAACCCTGCACACATTTCGT | Laloraya *et al.*, 2000 |

TABLE 2: Primers used in this study.

### SPI and microscopy

SPI screens were performed as previously described (Olafsson and Thorpe, 2015, 2018). Briefly, a universal donor strain, which contains conditional *GAL-CEN* centromeres, was transformed separately with the control and experimental plasmids (expressing either Cdc5-GBP, cdc5kd-GBP [a kinase-dead version], or GBP alone; all under the control of a constitutive *CUP1* promoter). These universal donor strains were then mated with members of the GFP collection arrayed with 16 replicates on 1536-colony rectangular agar plates using a pinning robot (ROTOR robot; Singer Instruments, UK). The resulting diploids were put through a series of sequential selection steps to maintain the plasmid, while destabilizing and then removing the chromosomes of the universal donor strain. The resulting plates were scanned using a desktop flatbed scanner (Epson V750 Pro; Seiko Epson Corporation, Japan). Colony sizes were assessed and the resulting data analyzed using the ScreenMill suite of software (Dittmar *et al.*, 2010). Flourescence imaging was performed on yeast cells embedded in 0.7% low-melting-point agarose dissolved in growth medium. The cells were imaged with a Zeiss Axioimager Z2 microscope using a 63× 1.4 NA oil immersion lens, illuminated with a Zeiss Colibri LED light source (GFP = 470 nm, RFP = 590 nm). Bright-field contrast was enhanced using differential interference prisms. Images were captured using a Flash 4.0 LT CMOS camera with 6.5 μm pixels binned 2 × 2 (Hamamatsu Photonics, Japan).

## ACKNOWLEDGMENTS

We are highly thankful to Sue Biggins, Orna Cohen-Fix, and Vincent Guacci for strains, plasmids, and helpful suggestions; Kathy McKinnon of the National Cancer Institute Vaccine Branch FACS Core for assistance with FACS; Mirela Pascariu for the purification of Cdc5 kinase; Timothy Waybright and Timothy Veenstra of the Frederick National Laboratory for Cancer Research for assistance with mass spectrometry; Pam Meluh for Mif2 antibodies; and the members of the Basrai laboratory for technical assistance and helpful discussions. P.K.M., L.B., T.J.W., Z.M.J., L.E.D., and M.A.B. were supported by the Intramural Research Program of the National Cancer Institute, National Institutes of Health; D.D. is supported by the Canadian Institutes of Health Research (MOP 82912, MOP 136788, PJT 148969) and by a Canada Research Chair in Chromatin Dynamics & Genome Architecture (Tier 1); and G.O. and P.H.T. were supported by the Queen Mary University of London and the Francis Crick Institute, which receives its core funding from Cancer Research UK (FC001003), the UK Medical Research Council (FC001003), and the Wellcome Trust (FC001003).

## REFERENCES

Akiyoshi B, Biggins S (2010). Cdc14-dependent dephosphorylation of a kinetochore protein prior to anaphase in *Saccharomyces cerevisiae*. Genetics 186, 1487–1491.

Alexandru G, Uhlmann F, Mechtler K, Poupart MA, Nasmyth K (2001). Phosphorylation of the cohesin subunit Scc1 by Polo/Cdc5 kinase regulates sister chromatid separation in yeast. Cell 105, 459–472.

Asano S, Park JE, Sakchaisri K, Yu LR, Song S, Supavilai P, Veenstra TD, Lee KS (2005). Concerted mechanism of Swe1/Wee1 regulation by multiple kinases in budding yeast. EMBO J 24, 2194–2204.

Au WC, Dawson AR, Rawson DW, Taylor SB, Baker RE, Basrai MA (2013). A novel role of the N-terminus of budding yeast histone H3 variant Cse4 in ubiquitin-mediated proteolysis. Genetics 194, 513–518.

Biggins S (2013). The composition, functions, and regulation of the budding yeast kinetochore. Genetics 194, 817–846.

Boeckmann L, Takahashi Y, Au WC, Mishra PK, Choy JS, Dawson AR, Szeto MY, Waybright TJ, Heger C, McAndrew C, *et al.* (2013). Phosphorylation of centromeric histone H3 variant regulates chromosome segregation in *Saccharomyces cerevisiae*. Mol Biol Cell 24, 2034–2044.

Botchkarev VV Jr, Haber JE (2018). Functions and regulation of the Polo-like kinase Cdc5 in the absence and presence of DNA damage. Curr Genet 64, 87–96.

Brooker AS, Berkowitz KM (2014). The roles of cohesins in mitosis, meiosis, and human health and disease. Methods Mol Biol 1170, 229–266.

Brown MT, Goetsch L, Hartwell LH (1993). MIF2 is required for mitotic spindle integrity during anaphase spindle elongation in *Saccharomyces cerevisiae*. J Cell Biol 123, 387–403.

Burrack LS, Berman J (2012). Flexibility of centromere and kinetochore structures. Trends Genet 28, 204–212.

Buvelot S, Tatsutani SY, Vermaak D, Biggins S (2003). The budding yeast Ipl1/Aurora protein kinase regulates mitotic spindle disassembly. J Cell Biol 160, 329–339.

Charles JF, Jaspersen SL, Tinker-Kulberg RL, Hwang L, Szidon A, Morgan DO (1998). The Polo-related kinase Cdc5 activates and is destroyed by the mitotic cyclin destruction machinery in *S. cerevisiae*. Curr Biol 8, 497–507.

Cheeseman IM, Anderson S, Jwa M, Green EM, Kang J, Yates JR 3rd, Chan CS, Drubin DG, Barnes G (2002). Phospho-regulation of kinetochore-microtubule attachments by the Aurora kinase Ipl1p. Cell 111, 163–172.

Chen Y, Baker RE, Keith KC, Harris K, Stoler S, Fitzgerald-Hayes M (2000). The N terminus of the centromere H3-like protein Cse4p performs an essential function distinct from that of the histone fold domain. Mol Cell Biol 20, 7037–7048.

Cho US, Corbett KD, Al-Bassam J, Bellizzi JJ 3rd, De Wulf P, Espelin CW, Miranda JJ, Simons K, Wei RR, Sorger PK, Harrison SC (2010). Molecular structures and interactions in the yeast kinetochore. Cold Spring Harb Symp Quant Biol 75, 395–401.

Cho WH, Lee YJ, Kong SI, Hurwitz J, Lee JK (2006). CDC7 kinase phosphorylates serine residues adjacent to acidic amino acids in the minichromosome maintenance 2 protein. Proc Natl Acad Sci USA 103, 11521–11526.

Choy JS, Acuna R, Au WC, Basrai MA (2011). A role for histone H4K16 hypoacetylation in *Saccharomyces cerevisiae* kinetochore function. Genetics 189, 11–21.

Clarke L, Carbon J (1980). Isolation of a yeast centromere and construction of functional small circular chromosomes. Nature 287, 504–509.

Cohen RL, Espelin CW, De Wulf P, Sorger PK, Harrison SC, Simons KT (2008). Structural and functional dissection of Mif2p, a conserved DNA-binding kinetochore protein. Mol Biol Cell 19, 4480–4491.

Dittmar JC, Reid RJ, Rothstein R (2010). ScreenMill: a freely available software suite for growth measurement, analysis and visualization of high-throughput screen data. BMC Bioinformatics 11, 353.

Eckert CA, Gravdahl DJ, Megee PC (2007). The enhancement of pericentromeric cohesin association by conserved kinetochore components promotes high-fidelity chromosome segregation and is sensitive to microtubule-based tension. Genes Dev 21, 278–291.

Haase J, Mishra PK, Stephens A, Haggerty R, Quammen C, Taylor RM 2nd, Yeh E, Basrai MA, Bloom K (2013). A 3D map of the yeast kinetochore reveals the presence of core and accessory centromere-specific histone. Curr Biol 23, 1939–1944.

Henikoff S, Ahmad K, Platero JS, van Steensel B (2000). Heterochromatic deposition of centromeric histone H3-like proteins. Proc Natl Acad Sci USA 97, 716–721.

Hewawasam G, Shivaraju M, Mattingly M, Venkatesh S, Martin-Brown S, Florens L, Workman JL, Gerton JL (2010). Psh1 is an E3 ubiquitin ligase that targets the centromeric histone variant Cse4. Mol Cell 40, 444–454.

Hinshaw SM, Makrantoni V, Harrison SC, Marston AL (2017). The kinetochore receptor for the cohesin loading complex. Cell 171, 72–84 e13.

Ho KH, Tsuchiya D, Oliger AC, Lacefield S (2014). Localization and function of budding yeast CENP-A depends upon kinetochore protein interactions and is independent of canonical centromere sequence. Cell Rep 9, 2027–2033.

Hoffmann G, Samel-Pommerencke A, Weber J, Cuomo A, Bonaldi T, Ehrenhofer-Murray AE (2018). A role for CENP-A/Cse4 phosphorylation on serine 33 in deposition at the centromere. FEMS Yeast Res 18, fox094.

Hornig NC, Uhlmann F (2004). Preferential cleavage of chromatin-bound cohesin after targeted phosphorylation by Polo-like kinase. EMBO J 23, 3144–3153.

Huh WK, Falvo JV, Gerke LC, Carroll AS, Howson RW, Weissman JS, O'Shea EK (2003). Global analysis of protein localization in budding yeast. Nature 425, 686–691.

Jin F, Bokros M, Wang Y (2017). The phosphorylation of a kinetochore protein Dam1 by Aurora B/Ipl1 kinase promotes chromosome bipolar attachment in yeast. Sci Rep 7, 11880.

Kastenmayer JP, Lee MS, Hong AL, Spencer FA, Basrai MA (2005). The C-terminal half of *Saccharomyces cerevisiae* Mad1p mediates spindle checkpoint function, chromosome transmission fidelity and CEN association. Genetics 170, 509–517.

Keith KC, Baker RE, Chen Y, Harris K, Stoler S, Fitzgerald-Hayes M (1999). Analysis of primary structural determinants that distinguish the centromere-specific function of histone variant Cse4p from histone H3. Mol Cell Biol 19, 6130–6139.

Laloraya S, Guacci V, Koshland D (2000). Chromosomal addresses of the cohesin component Mcd1p. J Cell Biol 151, 1047–1056.

Lang J, Barber A, Biggins S (2018). An assay for de novo kinetochore assembly reveals a key role for the CENP-T pathway in budding yeast. eLife 7, e37819.

Lechner J, Carbon J (1991). A 240 kd multisubunit protein complex, CBF3, is a major component of the budding yeast centromere. Cell 64, 717–725.

Livak KJ, Schmittgen TD (2001). Analysis of relative gene expression data using real-time quantitative PCR and the $2^{-\Delta\Delta C_T}$ method. Methods 25, 402–408.

Luger K, Rechsteiner TJ, Flaus AJ, Waye MM, Richmond TJ (1997). Characterization of nucleosome core particles containing histone proteins made in bacteria. J Mol Biol 272, 301–311.

McKinley KL, Cheeseman IM (2014). Polo-like kinase 1 licenses CENP-A deposition at centromeres. Cell 158, 397–411.

Meluh PB, Koshland D (1995). Evidence that the MIF2 gene of *Saccharomyces cerevisiae* encodes a centromere protein with homology to the mammalian centromere protein CENP-C. Mol Biol Cell 6, 793–807.

Meluh PB, Yang P, Glowczewski L, Koshland D, Smith MM (1998). Cse4p is a component of the core centromere of *Saccharomyces cerevisiae*. Cell 94, 607–613.

Mishra PK, Au WC, Choy JS, Kuich PH, Baker RE, Foltz DR, Basrai MA (2011). Misregulation of Scm3p/HJURP causes chromosome instability in *Saccharomyces cerevisiae* and human cells. PLoS Genet 7, e1002303.

Mishra PK, Baum M, Carbon J (2007). Centromere size and position in *Candida albicans* are evolutionarily conserved independent of DNA sequence heterogeneity. Mol Genet Genomics 278, 455–465.

Mishra PK, Ciftci-Yilmaz S, Reynolds D, Au WC, Boeckmann L, Dittman LE, Jowhar Z, Pachpor T, Yeh E, Baker RE, *et al.* (2016). Polo kinase Cdc5 associates with centromeres to facilitate the removal of centromeric cohesin during mitosis. Mol Biol Cell 27, 2286–2300.

Mishra PK, Ottmann AR, Basrai MA (2013). Structural integrity of centromeric chromatin and faithful chromosome segregation requires Pat1. Genetics 195, 369–379.

Mishra PK, Thapa KS, Chen P, Wang S, Hazbun TR, Basrai MA (2018). Budding yeast CENP-A(Cse4) interacts with the N-terminus of Sgo1 and regulates its association with centromeric chromatin. Cell Cycle 17, 11–23.

Musacchio A, Desai A (2017). A molecular view of kinetochore assembly and function. Biology (Basel) 6, 5.

Ng TM, Waples WG, Lavoie BD, Biggins S (2009). Pericentromeric sister chromatid cohesion promotes kinetochore biorientation. Mol Biol Cell 20, 3818–3827.

Ohkuni K, Takahashi Y, Fulp A, Lawrimore J, Au WC, Pasupala N, Levy-Myers R, Warren J, Strunnikov A, Baker RE, *et al.* (2016). SUMO-targeted ubiquitin ligase (STUbL) Slx5 regulates proteolysis of centromeric histone H3 variant Cse4 and prevents its mislocalization to euchromatin. Mol Biol Cell 27, 1500–1510.

Olafsson G, Thorpe PH (2015). Synthetic physical interactions map kinetochore regulators and regions sensitive to constitutive Cdc14 localization. Proc Natl Acad Sci USA 112, 10413–10418.

Olafsson G, Thorpe PH (2016). Synthetic physical interactions map kinetochore-checkpoint activation regions. G3 (Bethesda) 6, 2531–2542.

Olafsson G, Thorpe PH (2018). Rewiring the budding yeast proteome using synthetic physical interactions. Methods Mol Biol 1672, 599–612.

Ortiz J, Stemmann O, Rank S, Lechner J (1999). A putative protein complex consisting of Ctf19, Mcm21, and Okp1 represents a missing link in the budding yeast kinetochore. Genes Dev 13, 1140–1155.

Park CJ, Park JE, Karpova TS, Soung NK, Yu LR, Song S, Lee KH, Xia X, Kang E, Dabanoglu I, et al. (2008). Requirement for the budding yeast polo kinase Cdc5 in proper microtubule growth and dynamics. Eukaryot Cell 7, 444–453.

Pearson CG, Yeh E, Gardner M, Odde D, Salmon ED, Bloom K (2004). Stable kinetochore-microtubule attachment constrains centromere positioning in metaphase. Curr Biol 14, 1962–1967.

Pekgoz Altunkaya G, Malvezzi F, Demianova Z, Zimniak T, Litos G, Weissmann F, Mechtler K, Herzog F, Westermann S (2016). CCAN assembly configures composite binding interfaces to promote cross-linking of Ndc80 complexes at the kinetochore. Curr Biol 26, 2370–2378.

Phizicky DV, Berchowitz LE, Bell SP (2018). Multiple kinases inhibit origin licensing and helicase activation to ensure reductive cell division during meiosis. eLife 7, e33309.

Rahal R, Amon A (2008). The Polo-like kinase Cdc5 interacts with FEAR network components and Cdc14. Cell Cycle 7, 3262–3272.

Ranjitkar P, Press MO, Yi X, Baker R, MacCoss MJ, Biggins S (2010). An E3 ubiquitin ligase prevents ectopic localization of the centromeric histone H3 variant via the centromere targeting domain. Mol Cell 40, 455–464.

Ratsima H, Ladouceur AM, Pascariu M, Sauve V, Salloum Z, Maddox PS, D'Amours D (2011). Independent modulation of the kinase and polo-box activities of Cdc5 protein unravels unique roles in the maintenance of genome stability. Proc Natl Acad Sci USA 108, E914–E923.

Reid RJ, Gonzalez-Barrera S, Sunjevaric I, Alvaro D, Ciccone S, Wagner M, Rothstein R (2011). Selective ploidy ablation, a high-throughput plasmid transfer protocol, identifies new genes affecting topoisomerase I-induced DNA damage. Genome Res 21, 477–486.

Robellet X, Thattikota Y, Wang F, Wee TL, Pascariu M, Shankar S, Bonneil E, Brown CM, D'Amours D (2015). A high-sensitivity phospho-switch triggered by Cdk1 governs chromosome morphogenesis during cell division. Genes Dev 29, 426–439.

Roccuzzo M, Visintin C, Tili F, Visintin R (2015). FEAR-mediated activation of Cdc14 is the limiting step for spindle elongation and anaphase progression. Nat Cell Biol 17, 251–261.

Rossio V, Galati E, Ferrari M, Pellicioli A, Sutani T, Shirahige K, Lucchini G, Piatti S (2010). The RSC chromatin-remodeling complex influences mitotic exit and adaptation to the spindle assembly checkpoint by controlling the Cdc14 phosphatase. J Cell Biol 191, 981–997.

Rothbauer U, Zolghadr K, Muyldermans S, Schepers A, Cardoso MC, Leonhardt H (2008). A versatile nanotrap for biochemical and functional studies with fluorescent fusion proteins. Mol Cell Proteomics 7, 282–289.

Samel A, Cuomo A, Bonaldi T, Ehrenhofer-Murray AE (2012). Methylation of CenH3 arginine 37 regulates kinetochore integrity and chromosome segregation. Proc Natl Acad Sci USA 109, 9029–9034.

Santaguida S, Amon A (2015). Short- and long-term effects of chromosome mis-segregation and aneuploidy. Nat Rev Mol Cell Biol 16, 473–485.

Saunders MJ, Yeh E, Grunstein M, Bloom K (1990). Nucleosome depletion alters the chromatin structure of *Saccharomyces cerevisiae* centromeres. Mol Cell Biol 10, 5721–5727.

Schneider CA, Rasband WS, Eliceiri KW (2012). NIH Image to ImageJ: 25 years of image analysis. Nat Methods 9, 671–675.

Snead JL, Sullivan M, Lowery DM, Cohen MS, Zhang C, Randle DH, Taunton J, Yaffe MB, Morgan DO, Shokat KM (2007). A coupled chemical-genetic and bioinformatic approach to Polo-like kinase pathway exploration. Chem Biol 14, 1261–1272.

Spencer F, Gerring SL, Connelly C, Hieter P (1990). Mitotic chromosome transmission fidelity mutants in *Saccharomyces cerevisiae*. Genetics 124, 237–249.

Stoler S, Keith KC, Curnick KE, Fitzgerald-Hayes M (1995). A mutation in CSE4, an essential gene encoding a novel chromatin-associated protein in yeast, causes chromosome nondisjunction and cell cycle arrest at mitosis. Genes Dev 9, 573–586.

St-Pierre J, Douziech M, Bazile F, Pascariu M, Bonneil E, Sauve V, Ratsima H, D'Amours D (2009). Polo kinase regulates mitotic chromosome condensation by hyperactivation of condensin DNA supercoiling activity. Mol Cell 34, 416–426.

Strunnikov AV, Kingsbury J, Koshland D (1995). CEP3 encodes a centromere protein of *Saccharomyces cerevisiae*. J Cell Biol 128, 749–760.

Sullivan KF, Hechenberger M, Masri K (1994). Human CENP-A contains a histone H3 related histone fold domain that is required for targeting to the centromere. J Cell Biol 127, 581–592.

Takahashi K, Chen ES, Yanagida M (2000). Requirement of Mis6 centromere connector for localizing a CENP-A-like protein in fission yeast. Science 288, 2215–2219.

Tsabar M, Haase J, Harrison B, Snider CE, Eldridge B, Kaminsky L, Hine RM, Haber JE, Bloom K (2016). A cohesin-based partitioning mechanism revealed upon transcriptional inactivation of centromere. PLoS Genet 12, e1006021.

Tukenmez H, Magnussen HM, Kovermann M, Bystrom A, Wolf-Watz M (2016). Linkage between fitness of yeast cells and adenylate kinase catalysis. PLoS One 11, e0163115.

Uhlmann F, Wernic D, Poupart MA, Koonin EV, Nasmyth K (2000). Cleavage of cohesin by the CD clan protease separin triggers anaphase in yeast. Cell 103, 375–386.

Van Hooser AA, Ouspenski II, Gregson HC, Starr DA, Yen TJ, Goldberg ML, Yokomori K, Earnshaw WC, Sullivan KF, Brinkley BR (2001). Specification of kinetochore-forming chromatin by the histone H3 variant CENP-A. J Cell Sci 114, 3529–3542.
Verdaasdonk JS, Bloom K (2011). Centromeres: unique chromatin structures that drive chromosome segregation. Nat Rev Mol Cell Biol 12, 320–332.
Verdaasdonk JS, Gardner R, Stephens AD, Yeh E, Bloom K (2012). Tension-dependent nucleosome remodeling at the pericentromere in yeast. Mol Biol Cell 23, 2560–2570.
Walters AD, May CK, Dauster ES, Cinquin BP, Smith EA, Robellet X, D'Amours D, Larabell CA, Cohen-Fix O (2014). The yeast polo kinase Cdc5 regulates the shape of the mitotic nucleus. Curr Biol 24, 2861–2867.
Waybright T, Gillette W, Esposito D, Stephens R, Lucas D, Hartley J, Veenstra T (2008). Identification of highly expressed, soluble proteins using an improved, high-throughput pooled ORF expression technology. Biotechniques 45, 307–315.
Weber SA, Gerton JL, Polancic JE, DeRisi JL, Koshland D, Megee PC (2004). The kinetochore is an enhancer of pericentric cohesin binding. PLoS Biol 2, E260.
Westermann S, Cheeseman IM, Anderson S, Yates JR 3rd, Drubin DG, Barnes G (2003). Architecture of the budding yeast kinetochore reveals a conserved molecular core. J Cell Biol 163, 215–222.
Widlund PO, Davis TN (2005). A high-efficiency method to replace essential genes with mutant alleles in yeast. Yeast 22, 769–774.
Yeh E, Haase J, Paliulis LV, Joglekar A, Bond L, Bouck D, Salmon ED, Bloom KS (2008). Pericentric chromatin is organized into an intramolecular loop in mitosis. Curr Biol 18, 81–90.
Zitouni S, Nabais C, Jana SC, Guerrero A, Bettencourt-Dias M (2014). Polo-like kinases: structural variations lead to multiple functions. Nat Rev Mol Cell Biol 15, 433–452.